



AFRPL TR-83-053

AD:



Final Report
for the period
11 June 1979 to
10 March 1982

Shock Tube Study of the Ignition and Combustion of Aluminum

AD-A234033

August 1983

Authors:

J. F. Driscoll

J. A. Nicholls

V. Patel

B. Khatib-Shahidi

T. C. Liu

Department of Aerospace Engineering

The University of Michigan

Ann Arbor, Michigan 48109

F04611-79-C-0030

UM-017385-F

Approved for Public Release

Distribution unlimited. The AFRPL Technical Services Office has reviewed this report, and it is releasable to the National Technical Information Service, where it will be available to the general public, including foreign nationals.

DTIC
ELECTED
OCT 26 1983
S D

prepared for the: **Air Force
Rocket Propulsion
Laboratory**

D

Air Force Space Technology Center
Space Division, Air Force Systems Command
Edwards Air Force Base,
California 93523

FILE COPY
TM

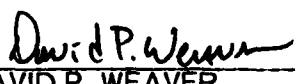
NOTICES

When U.S. Government drawings, specifications, or other data are used for any purpose other than a definitely related Government procurement operation, the fact that the Government may have formulated, furnished, or in any way supplies the said drawings, specifications, or other data, is not to be regarded by implication or otherwise, or in any manner licensing the holder or any other person or corporation, or conveying any rights or permission to manufacture, use, or sell any patented invention that may be related thereto.

FOREWORD

This report was submitted by the University of Michigan, Department of Aerospace Engineering, Gas Dynamics Laboratory under Contract F04611-79-C-0030, Job Order No. 2308MIUE with the Air Force Rocket Propulsion Laboratory, Edwards AFB CA 93523.

This Final Report is approved for release and publication in accordance with the distribution statement on the cover and on the DD Form 1473.


DAVID P. WEAVER

Project Manager


WILBUR C. ANDREPONI
Chief, Plume Technology Branch

FOR THE DIRECTOR


ROBERT L. GEISLER
Deputy Chief, Propulsion Analysis Division

UNCLASSIFIED

SECURITY CLASSIFICATION OF THIS PAGE (When Data Entered)

REPORT DOCUMENTATION PAGE		READ INSTRUCTIONS BEFORE COMPLETING FORM
1. REPORT NUMBER AFRPL-TR-83-053	2. GOVT ACCESSION NO.	3. RECIPIENT'S CATALOG NUMBER
4. TITLE (and Subtitle) SHOCK TUBE STUDY OF THE IGNITION AND COMBUSTION OF ALUMINUM		5. TYPE OF REPORT & PERIOD COVERED Final 11 June 1979-10 March 1982
7. AUTHOR(s) J.F. Driscoll V. Patel J.A. Nicholls B. Katib-Shahidi T.C. Liu		6. PERFORMING ORG. REPORT NUMBER UM 017385-F 8. CONTRACT OR GRANT NUMBER(s) F04611-79-C-0030
9. PERFORMING ORGANIZATION NAME AND ADDRESS Gas Dynamics Laboratories Dept. Aerospace Engineering The University of Michigan Ann Arbor, MI 48109		10. PROGRAM ELEMENT, PROJECT, TASK AREA & WORK UNIT NUMBERS
11. CONTROLLING OFFICE NAME AND ADDRESS Air Force Rocket Propulsion Laboratory/ DYP Stop 24 Edwards AFB, California 93523		12. REPORT DATE August 1983
14. MONITORING AGENCY NAME & ADDRESS (if different from Controlling Office) ONRRR Ohio State University Research Center 1314 Kinnerar Road Columbus, OH 43212		13. NUMBER OF PAGES 72
16. DISTRIBUTION STATEMENT (of this Report) Approved for Public Release; Distribution Unlimited		15. SECURITY CLASS. (of this report) Unclassified
17. DISTRIBUTION STATEMENT (of the abstract entered in Block 20, if different from Report)		
18. SUPPLEMENTARY NOTES		
19. KEY WORDS (Continue on reverse side if necessary and identify by block number) Metal Combustion Ignition Aluminum		
20. ABSTRACT (Continue on reverse side if necessary and identify by block number) Addition of aluminum to solid rocket propellants can significantly improve performance but may seriously increase plume visibility and radiative heating of the nozzle. The goal of this project is to obtain data that will help identify the reaction mechanism and the ignition limits of aluminum at elevated temperatures and pressures. Formidable problems arise when attempting such measurements in rocket		

UNCLASSIFIED

SECURITY CLASSIFICATION OF THIS PAGE(When Data Entered)

motors since conditions are unsteady and not easy to control. Therefore, it was decided to mount a pure aluminum sample to the end wall of a shock tube and to ignite the sample using a reflected shock wave. The pressures and temperatures that can be achieved (40 atm, 5000°K) are typical of rocket motor conditions and are much higher than those obtained in previous studies using incident shock waves in conventional shock tubes. The aluminum sample reacts with a test gas in which the proportions of nitrogen, hydrogen, oxygen and chlorine are the same as found in ammonium perchlorate.

A single pulse shock tube was designed and constructed; proper techniques to carefully ignite the aluminum were determined. The reaction surface was photographed using a high speed movie camera. Ignition of the aluminum sample occurred for temperatures above 2400K.

A number of intermediate species were detected in the Al-N₂-H₂-Cl₂-O₂ reaction at 40 atm., 5000K using emission spectroscopy. Species that were conclusively identified were Al, Al+, AlO, H₂O, O⁺, and N. Other weak emission bands were believed due to AlH, OH, AlOH or AlCl. Time histories of the AlO emission band indicate that AlO reaches a maximum before the continuum radiation reaches a maximum, which is an indicator, but not positive proof, that AlO is a precursor to Al₂O₃ in the reaction scheme.

Solid products of combustion were analyzed using a transmission electron microscope, electron diffraction, and X-Ray diffraction techniques. Spherical Al₂O₃ particles were observed in the 0.1 to 1 μm size range. The major products were Al₂O₃, HCl, and H₂O as expected, with the latter two products causing appreciable agglomeration of the Al₂O₃ particles. No traces of NH₄Cl, AlCl₃ or NH₃ were found.

Gaseous HCl and H₂O were detected using infrared spectrometry to analyze the end gas. Levels of NO and NO₂ were more than 10,000 times larger than the predicted equilibrium concentrations, indicating that significant deviations from the equilibrium NO chemistry occurred.

UNCLASSIFIED

SECURITY CLASSIFICATION OF THIS PAGE(When Data Entered)

PREFACE

Dr. David Weaver of the Rocket Propulsion Lab, Edwards AFB, has been Technical Monitor of this research effort; previously Dr. David M. Mann served as Technical Monitor. The study has been conducted in the Gas Dynamics Laboratories, Department of Aerospace Engineering, The University of Michigan, under the direction of Professor J.A. Nicholls and with Professor J.F. Driscoll as the Principal Investigator. V. Patel and B. Khatib-Shahidi were graduate students associated with the project; Dr. T.C. Liu was a Visiting Scientist.

Accession For	
NTIS GRA&I	<input checked="" type="checkbox"/>
DTIC TAB	<input type="checkbox"/>
Unannounced	<input type="checkbox"/>
Justification	
By _____	
Distribution/	
Availability Codes	
Dist	Avail and/or Special
A	

NTIS COPY INSPECTED 2

TABLE OF CONTENTS

	Page
ABSTRACT	ii
PREFACE	iv
LIST OF FIGURES	vi
I. INTRODUCTION	1
II. RESEARCH GOALS	4
III. EXPERIMENTAL FACILITY	5
A. Design and Instrumentation	5
B. Range of Run Conditions	10
C. Operating Procedure	11
IV. RESULTS	13
A. Ignition of Aluminum in Oxygen	13
B. Calculation of Possible Species Present	14
C. Spectrographic Results	16
D. Chemical Kinetics	18
E. Solid and Gaseous Combustion Products	21
V. CONCLUSIONS	25
VI. RECOMMENDATIONS	27
VII. REFERENCES	28

LIST OF FIGURES

	Page
Figure 1. Schematic of the Reaction Zone Near (a) An Aluminum Particle in a Rocket Motor and (b) An Aluminum Sample in the Shock Tube	30
Figure 2. Schematic of the Chemical Kinetic Shock Tube	31
Figure 3. Photograph of the Shock Tube	32
Figure 4. Schematic of Thermal Boundary Layer Near Sample	33
Figure 5. Typical Shock Tube Operating Conditions	34
Figure 6. Gas Pressure Behind Reflected Shock Just Prior to Sample Ignition; Real Gas Effects Included in Gordon-McBride Program	35
Figure 7. Gas Temperature Behind Reflected Shock Just Prior to Sample Ignition; Real Gas Effects Included in Gordon-McBride Program	36
Figure 8. Composition of the Gas Behind the Reflected Shock Just Prior to Sample Ignition; Real Gas Effects Included	37
Figure 9. Ratio of Specific Heats (γ) and Molecular Weight of Gas Just Prior to Ignition	38
Figure 10. Run Condition for Pure Oxygen — NASA CEC Program Checked for Proper Convergence	40
Figure 11. Equilibrium Concentrations of Species for $\text{Al}-\text{O}_2$ Reaction	41
Figure 12. Oscilloscope Traces Showing (a) Pressure History at End Wall; (b) Pressure History Two Meters from End Wall	42
Figure 13. Photograph of the Ignition of the Aluminum Sample Mounted on Shock Tube End Wall	43
Figure 14. High Speed Movie of the Aluminum Sample Ignition Process	44
Figure 15. Aluminum Ignition Data for Various Pressure and Temperatures in Oxygen	45
Figure 16. Calculated Mole Fractions of Various Species in the $\text{Al}-\text{O}_2-\text{N}_2-\text{Cl}_2-\text{H}_2$ Reaction at 4360 K	46

LIST OF FIGURES (concluded)

	Page
Figure 17. Other Species Considered in the Calculations Whose Mole Fractions were Less than 5×10^{-6}	50
Figure 18. Variation of Reaction Products as Temperature Decreases to 300 K	51
Figure 19. Comparison of Computed Equilibrium Products for the $\text{NH}_4\text{ClO}_4\text{-Al}$ Reaction with those for the $.1 \text{ N}_2 + .4 \text{ H}_2 + .1 \text{ Cl}_2 + .4 \text{ O}_2\text{-Al}$ Reaction	53
Figure 20. Effect of Increasing Aluminum Content on the Calculated Adiabatic Flame Temperature of a $\text{NH}_4\text{ClO}_4\text{-Al}$ Flame	54
Figure 21. Emission Spectrum of Aluminum-Oxygen Reaction in the Shock Tube	55
Figure 22. Emission Spectra of the Reaction of Aluminum with Various Gas Mixtures in the Shock Tube	56
Figure 23. Spectra of Reference Lamps Used	57
Figure 24. Time History of Emission Spectra	58
Figure 25. Transmission Electron Micrograph of Al_2O_3 Formed in Shock Tube	59
Figure 26. Scanning Electron Micrograph and X-ray Diffraction Analysis of Solid Products of Combustion	60
Figure 27. Upper Curve: Analysis of Solids Products of A O_2 Reaction Using X-ray Diffraction, Indicating Presence of Al_2O_3 ; Bottom Photo: Similar Result Using Electron Diffraction	61
Figure 28. Electron Micrograph and X-Ray Diffraction Analysis of Products of $\text{Al} + \text{N}_2 + \text{H}_2 + \text{Cl}_2 + \text{O}_2$ Reaction	62
Figure 29. Magnified View of Chlorine Containing Region	63
Figure 30. Infrared Spectrometer Analysis of Gaseous Products	64

I. INTRODUCTION

Aluminum remains the most common metal that is used to improve the performance of solid propellants for rocket motors¹⁻⁶. In spite of many years of study, there still exist many questions in connection with its use. The exact chemical kinetic steps involved in the aluminum-oxygen reaction are still debated, even for low pressures, i.e. below one atmosphere where most of the kinetics research has been conducted; virtually no fundamental chemical kinetic data has been obtained for pressures above 10 atm. The mechanism by which the solid combustion product Al_2O_3 condense and agglomerates is not sufficiently well understood. As a consequence, problems exist when using computer codes to assist in rocket motor design because of difficulties in predicting two phase flow effects. Three important detrimental effects of Al_2O_3 particulates are the two phase flow losses which reduce the specific impulse, the increased radiative heating of the nozzle due to particulates, and the increased plume visibility. It is desirable to reduce these three effects while continuing to use aluminum, which helps to optimize performance and to reduce combustion instabilities.

→ The motivation for the present research project has been the need to obtain fundamental data relating to aluminum combustion in a controlled environment in the pressure range up to 40 atm and the temperature range up to 5000 K, typical of rocket motor conditions. Previous work in controlled laboratory experiments has been confined to pressures less than approximately 10 atm, using such devices as flow reactors, burning ribbons, laser heating, and incident shock waves in shock tubes. ←

For example, a fast flow reactor produces a laminar, pre-mixed aluminum vapor/oxygen flat flame which is several centimeters thick and ideal for kinetics studies. Unfortunately, the pressure must be maintained below 0.1 atm, and the resulting

premixed flame is not likely to be representative of the diffusion flames that actually occur around burning aluminum particles in rocket motors. Burning ribbons and incident shock wave studies generally have been limited to pressures below 10 atm. Using incident shock waves, aluminum particles are quickly accelerated in a shock tube, and conditions near the moving particle are difficult to ascertain. Convective effects that dominate such processes were not of interest in the present study.

To obtain the fundamental information that was desired, it was decided that the operation of an actual rocket motor would not be feasible. Because of the formidable problems of a moving reaction surface, three dimensional flow field, and the motion of the aluminum particles of interest, it was decided to use a shock tube instead.

The primary region of interest is the reaction zone that occurs near the surface of a burning aluminum particle, which is shown schematically in Fig. 1. To simulate this reaction zone, it was decided to mount an aluminum sample on the end wall of a shock tube, and subject the sample to a strong reflected shock wave as shown schematically in Fig. 1. This technique offers the following advantages over previously used methods.

- a) The aluminum surface is essentially stationary, the reaction zone is large enough (2 cm by 2 cm) and the test time long enough (10 msec) to allow spectroscopic techniques to be used.
- b) Pressures up to 40 atm are easily controlled and measured, and are uniform in the reaction zone; likewise the gas temperature prior to ignition can be measured and controlled up to 5000 K. These pressures and temperatures are considerably higher than used in previous studies, including previous shock tube work.

- c) Gas composition is easily varied; initially pure oxygen was used; later a mixture of .1 N₂ + .4 H₂ + .1 Cl₂ + .4 O₂ was used because it has the same elemental composition as ammonium perchlorate⁷ (NH₄ClO₄).
- d) Solid and gas phase combustion products are easily collected and analyzed.

The research conducted is outlined in the following sections. The research goals are summarized, and the design, performance capability and operating procedure for the shock tube facility are described. Specific results and conclusions follow.

II. RESEARCH GOALS

The goals of the study were:

1. To build single pulse chemical kinetic shock tube and to obtain a diffusion flame near the surface of a burning aluminum sample at 40 atm pressure and a temperature of 5000 K in order to simulate conditions that would occur near a burning aluminum particle in a rocket motor.
2. To design conditions such that the sample size (2 cm x 2 cm) and test time (10 msec) are sufficiently large to study the reaction zone spectroscopically.
3. To determine the ignition temperature of the sample for a range of pressures.
4. To photograph the reaction process using a high speed framing camera.
5. To use emission spectroscopy to identify intermediate species in the $\text{Al} + \text{O}_2$ reaction and in the $\text{Al} + .1 \text{ N}_2 + .4 \text{ H}_2 + .1 \text{ Cl}_2 + .4 \text{ O}_2$ reaction at 40 atm, 5000 K.
6. To compare observed species with the 39 possible intermediate species predicted by the NASA Chemical Equilibrium Program for the $\text{Al-N}_2\text{-H}_2\text{-Cl}_2\text{-O}_2$ reaction.
7. To record the time history of the emitted spectral bands corresponding to AlO and to the background continuum, in the attempt to provide information concerning the sequence of reaction steps.
8. To analyze the solid products of combustion using electron microscope, electron diffraction, and X-ray diffraction methods.
9. To analyze the gaseous products of combustion using infrared absorption gas analysis.

III. EXPERIMENTAL FACILITY

A. Design and Instrumentation

The shock tube shown schematically in Figure 2 is designed to allow for single pulse, "tailored" conditions, similar to those achieved by Brabbs⁸ at NASA and Bauer⁹ at Cornell. It consists of a 14 ft long stainless steel driver section (3.5 in. OD, .30 in. wall) and a 20 ft long driven section (3.5 in. x 2.5 in., .30 in. wall). Photographs of the tube are shown in Figure 3. The driver tube has circular cross section in order to withstand driver pressures up to 3000 psi; the driven tube is rectangular so that the windows that are mounted near the end wall are flush with the sidewalls. In this way the windows will not disturb the shock wave near the end wall. Between the circular driver and rectangular driven tube there is a one foot long transition section, machined from stainless steel, which provides a gradual change in the inner wall from circular to rectangular.

To the left of the driver tube shown in Figure 2 are two other driver tube sections which are removable. A pipe elbow connects these sections to a large 40 ft long vacuum tank. The purpose of these removable driver tube lengths is to allow for "tailored" shock tube conditions in order to maximize the test time. The effective test time available is labeled on the t-x diagram of Figure 2. When the primary diaphragm is broken, the incident shock reflects off the end wall causing the aluminum sample on the end wall to ignite. Meanwhile, expansion waves reflect off the secondary diaphragm and eventually reflect off the end wall of the tube. This quenches the reaction at the end wall. In addition, the interface between the driver gas (helium) and the driven gas (O_2 , N_2 , Cl_2 , H_2) may reflect off the end wall which also quenches the reaction. For any given run condition, the length of the driver tube can be varied to maximize testing time. The secondary diaphragm can be

broken using an exploding wire at some time after the expansion wave has reflected off of it, in order to prevent further reheating of the sample. In many cases this is not necessary since the gas in contact with the aluminum sample at this later time is primarily helium, thus the reaction is forever quenched.

It was decided to use .007 in. thick sheets of steel for the primary diaphragm. A number of materials were tested; mylar was first used because it is inexpensive and easy to cut, however, small fragments of mylar were found to break off when the diaphragm ruptured and later hit the aluminum sample during the combustion process. Similarly, aluminum diaphragms were found to fragment slightly, and the particles that broke off the diaphragm were observed to burn in the test section region near the end wall when no aluminum sample was used. With .007 in. thick steel diaphragms, no fragment broke off the diaphragm. The steel diaphragms that were subsequently used for all runs were scribed to the desired thickness so as to rupture at the proper driver pressure.

It was found that a mechanism to initiate the shock wave upon electrical command was needed. By simply raising the driver pressure slowly, one cannot predict exactly when the diaphragm will rupture. Therefore the driver pressure was set to a value just below the diaphragm rupture level. Upon electrical command, a solenoid valve would open, dumping additional driver gas into the driver section, causing the diaphragm to rupture almost immediately. This technique made the operation of the shock tube very dependable and allowed for proper synchronization with cameras and with pre-heating of the aluminum sample.

The aluminum sample (2 cm x 2 cm x .1 cm) was mounted on two copper electrodes which formed the end wall of the shock tube, as seen in Figure 2. Various mounting arrangements

were tested. Since the test time available is 10 msec, it is imperative that the thermal inertia of the sample be small enough so that the sample surface will reach the temperature of the gas behind the shock wave in much less than 1 msec. This was accomplished by preheating the sample to about 700 K by passing a DC current through it. Initially a current pulse was passed through the sample, using a capacitor discharge circuit, but the rapid heating of the foil caused it to melt along a thin line, thus opening the electrical circuit. A DC current caused the sample to heat uniformly until it glowed red, whereupon the shock wave was initiated.

The temperature of the aluminum sample depends on the thermal properties of material on which it is mounted. As shown in Fig. 4, at time $t = 0$ a temperature discontinuity at the end wall occurs, with the aluminum surface that is in contact with the gas experiencing the gas temperature while the surface in contact with the wall remains at the wall temperature, 300 K. After time zero, a thermal boundary layer propagates to the left in Fig. 4 having thickness $\delta_g = \sqrt{\alpha_g t}$ where α_g is the thermal diffusivity of the gas. A thermal boundary layer of thickness $\delta_w = \sqrt{\alpha_w t}$ also propagates to the right through the solid wall, which has thermal diffusivity α_w . Equating heat flux from the gas to heat flux to the wall, as done in Fig. 4 results in a temperature at the gas-wall interface of:

$$T_{Al} = \frac{\frac{k_g}{\sqrt{\alpha_g}} T_g + \frac{k_w}{\sqrt{\alpha_w}} 300 \text{ K}}{\frac{k_g}{\sqrt{\alpha_g}} + \frac{k_w}{\sqrt{\alpha_w}}}$$

Thus if the aluminum sample is mounted on a good insulator, $k_w/\sqrt{\alpha_w} \ll k_g/\sqrt{\alpha_g}$ and the aluminum temperature will always remain near T_g (i.e. above 4000 K) whereas if the aluminum sample is mounted directly on a metal wall, $k_w/\sqrt{\alpha_w} \gg k_g/\sqrt{\alpha_g}$ and the aluminum temperature will remain near 300 K.

Various ways to mount the aluminum sample were tested. Initially the sample was mounted on a Pyrex glass plate; even more structural rigidity could be obtained by vacuum depositing aluminum on the glass plate. In another test, the aluminum plate was mounted horizontally, parallel to the horizontal shock tube axis, so that high temperature gas is in contact with both sides of the aluminum. Optimum design was achieved by mounting the aluminum sample vertically 2 mm from the end wall. In this way high temperature gas surrounds the sample, whose thermal inertia is such that the aluminum reaches the gas temperature in less than 1 msec.

While Fig. 4 depicts the thermal boundary layer that exists with no combustion, the temperature profiles are significantly different from those shown in Fig. 4 when combustion occurs. The thermal boundary layer should have no effect on ignition, which occurs before the boundary layer has had time to grow. After ignition the thermal boundary layer should cause the flame temperatures to be less than the adiabatic flame temperature, but should not affect the fundamental conclusions of this study. A numerical model of the heat losses from the flame was developed to assist in shock tube design.

The test gas that is used is a mixture of 40% H_2 , 40% O_2 , 10% Cl_2 , 10% N_2 which is the ratio of H, O, Cl, N atoms in ammonium perchlorate (NH_4ClO_4). Initially it was planned to use ammonium (NH_3) and chlorine (Cl_2) but it was found that a mixture of these gases at room temperature underwent a reaction to form a whitish powder, believed to be NH_4Cl , ammonium chloride. Another possibility that was considered was to mix perchloric acid ($HClO_4$) with ammonia (NH_3); these species are the species that ammonium perchlorate decomposes into just before the flamefront in an ammonium perchlorate flame. However it was not known if these species are stable if mixed at room temperature, so, to minimize handling problems, it was decided to mix pure H_2 , O_2 , Cl_2 and N_2 , which was found to be stable.

The shock tube is instrumented with pressure transducers, pressure gauges, a photographic system, and a spectrometer. The pressure transducers are PCB 102A04 and 102A15 quartz stress-gauge transducers designed for pressures up to 1000 psi. These devices are used with an oscilloscope to record the pressures P_2 and P_5 which occur behind the incident and the reflected shock, respectively. A HP 5314A time interval counter measures the time between pulses output by two transducers two meters apart, so that incident shock velocities and reflected shock velocities are measured.

Pressure gauges were integrated into an elaborate stainless steel piping system with 20 high pressure valves to enable the various test gases to be properly mixed and introduced at the proper initial pressure.

The photographic system consisted of a Fastax 16 mm movie camera, a Polaroid camera for long time exposure photographs and a series of lenses to magnify the test section region. Development of all movie film was done immediately after the run by the graduate students and a technician.

The spectrometer used to record emission spectra was a GCA 215.5 half meter polychromator. This is a sophisticated \$20,000 diffraction grating instrument used in the department for many types of spectrographic work. Since the combustion events were pulsed and not steady state and low levels of light detection were required, ASA 3000 film was used to cover the visible spectrum. Various types of IR and UV film were considered, but were not believed to be fast enough to be of use. Various lenses were used with the polychromator but best signal levels were achieved with no lenses when the ratio of sample height to distance from the spectrometer slit was 9, which corresponded to the f number of the spectrometer.

B. Range of Run Conditions

The initial series of runs were made to determine the range of run conditions achievable in the shock tube. To measure the run conditions, the end wall pressures P_2 and P_5 which correspond to gas pressures behind the incident shock and the reflected shock were measured. The incident and reflected shock speeds u_i and u_r were measured using pressure transducers mounted two meters apart. Finally, the driver gas pressure P_4 was measured using a pressure gauge. These measurements are redundant so that one measurement can be used to check the accuracy of other measurements. From the pressure and velocity measurements, all the properties of the gas mixture behind the reflected shock wave (i.e. P_5 , T_5 , etc.) can be calculated. These conditions are the conditions that the aluminum is exposed to just prior to ignition.

To determine T_5 , the molecular weight M_5 and other gas conditions just prior to ignition, the NASA Equilibrium Gas Composition Program developed by Gordon and McBride was used. This computer program accounts for real gas effects (dissociation and reaction of the test gases - N_2 , O_2 , H_2 , Cl_2) and predicts the gas conditions behind the reflected shock wave. The typical conditions achievable are shown in Figures 5 to 11.

The maximum pressure and temperature conditions used in this study are tabulated in Figure 5 and plotted in Figures 6 and 7. These conditions correspond to 40 atm and 5000 K and an incident shock Mach number of 10.5. The driver gas pressure

was approximately 1500 psi. The shock tube is designed for operation up to 3000 psi but no runs with driver pressures above 1500 psi were attempted. Most runs were made at the conditions labeled "typical" in Figures 5, 6, and 7 because of the lower driver pressure (~ 400 psi) required and the reduced amount of helium required. At typical run conditions, the incident shock Mach number is 7.8, resulting in a pressure P_5 of 14.6 atm and a temperature T_5 of 4150 K behind the reflected shock. The initial gas mixture of 40% H_2 , 40% O_2 , 10% Cl_2 , and 10% N_2 dissociates and reacts to form the fourteen species listed in Figure 8 with their appropriate mole fractions. The molecular weight of this mixture at 4150 K is 25.67 g/mole and the ratio of specific heats γ is 1.117. These represent gas conditions just prior to ignition.

Before the above run conditions were finally deduced from the pressure measurements, the Gordon-McBride computer program was extensively checked out for proper convergence. The pressure P_5 and temperature T_5 behind the reflected shock were computed for air only and were compared with values tabulated by Bernstein¹⁰. Figures 10 and 11 show that proper convergence was achieved.

C. Operating Procedure

The following steps are necessary for each run of the shock tube:

1. Solid products left in the driven tube from the previous run must be carefully removed using a solvent and a sponge tied to a 25 ft long rod. (Any solvent on the walls is later removed by outgassing the tube.) At regular intervals, shock waves in pure oxygen (with no aluminum) are initiated to clean off the tube inner walls.
2. A steel diaphragm which has been scribed to the desired depth is inserted between driver and driven tubes.

3. The electrodes which form the tube end wall are cleaned and a new aluminum sample is carefully inserted and clamped at the edges. The electrodes must be filed between each run to insure good electrical contact with the sample.
4. The driven tube is evacuated and outgassed for thirty minutes.
5. The driven gas (H_2 , N_2 , Cl_2 , O_2) which has been previously mixed in a mixing tank is introduced into the driven tube.
6. The triggering levels of the transducers, time interval counters, and oscilloscopes are checked.
7. The driver tube is filled to the desired level, usually 400 psi of helium.
8. The surge tank is filled to a somewhat higher pressure, generally 600 psi of helium.
9. With the room lights out, film is loaded into the spectrometer and the entrance slit is opened. The long time exposure camera shutter is opened, if desired.
10. The DC current through the aluminum sample is slowly increased until the sample just begins to glow red.
11. Immediately the shock wave is initiated by depressing an electrical switch to open a solenoid valve which dumps the gas in the surge tank into the driver tube, which ruptures the diaphragm.
12. After the run a sample of the end gas is collected in an evacuated bottle.
13. The remaining gases are vented outside the building and the end flange is removed. A sample of the solid products of combustion is collected.

IV. RESULTS

A. Ignition of Aluminum in Oxygen

The ignition and combustion of the aluminum sample in a pure oxygen environment was studied first. The pressure history of the gas adjacent to the aluminum sample was recorded for every run, using a pressure transducer mounted 2 cm from the end wall of the shock tube. A typical pressure trace is shown in Figure 12. Run conditions for this trace were: Helium driver pressure = 400 psi; oxygen initial pressure = 20 mm Hg; incident shock strength = Mach 7; pressure behind reflected shock = 13 atm; temperature behind reflected wave = 4100 K. As the pressure trace of Figure 12 shows, the reflection of the shock off the end wall causes the gas pressure near the aluminum sample to rise from 20 mm Hg to 13 atm in this case. A small pressure disturbance is noted just after the shock reflection which is due to the presence of a small gap between the edge of the aluminum sample and the shock tube inner wall. This gap is necessary to keep the aluminum sample electrically isolated from the shock tube. When the electrodes and sample are removed, the pressure disturbance is not observed. The pressure trace shown in Figure 12b was obtained using a pressure transducer mounted two meters from the end wall. It clearly shows the gas pressure rising to a value P_2 behind the incident shock and later to a value P_5 behind the reflected shock.

Figure 13 is a photograph of the ignition of the aluminum sample taken with a long time exposure. The incident shock has traveled from the right to the left and has reflected back from the left to the right. Some hot gases are seen to pass through a thin horizontal gap between the electrodes. Some hot particles, either Al or Al_2O_3 are seen to travel to the right, away from the reaction zone. These particles may be emitted due to boiling of the aluminum at the sampling surface,

caused by gaseous impurities in the aluminum, as proposed by Glassman⁶. The particles may simply be aluminum sheared off the sample by the force of the shock wave reflection. Aluminum and condensed Al_2O_3 drops or particles contribute black body radiation which interferes with spectroscopic measurements. Figure 14 shows a motion picture sequence of the ignition process. A Fastax camera was operated at 5000 frames per second for these photographs.

Low temperature runs in the range $T_5 = 1600 - 3200$ K were made to determine the ignition temperature of aluminum. Data shown in Figure 15 shows that when the sample is exposed to pure oxygen at temperatures below 2000 K, no ignition was observed. When the oxygen temperature was above 2400 K, ignition occurred on every run. For oxygen temperatures between 2000 and 2400 K, the small particles emitted from the sample emitted bluish-white light and were believed to ignite. The bluish-white light is an indication of the existence of AlO . Therefore it is believed that no unique ignition temperature exists, although ignition does occur in the range 2000 - 2400 K. The ignition process is controlled primarily by the melting of the oxide layer, which is generally less than one micron thick and has a melting temperature of 2300 K. As the oxide layer reaches the melting point, any aerodynamic stripping of this oxide layer would aid in the ignition process, and may be the reason why the smaller moving particles are observed to ignite when the large sample does not.

B. Calculation of Possible Species Present

Because up to 80 species may be present in the reaction of $\text{Al}-\text{H}_2-\text{Cl}_2-\text{O}_2$ and N_2 , it was decided to perform some calculations prior to the analysis of emission spectra and end gases.

The gas conditions just before the ignition of the aluminum sample were calculated using the NASA CEC computer program written by Gordon and McBride. For the typical case of a

Mach 7.8 incident shock wave in a gas mixture of 40% H₂, 40% O₂, 10% Cl₂, 10% N₂ which corresponds to the elemental composition of ammonium perchlorate, the calculated gas conditions were given in Figure 8. No aluminum reactions were considered in these pre-ignition calculations.

In order to have some idea of the various species that might exist after the aluminum has ignited, the Gordon and McBride program was run using the previously calculated gas conditions as initial conditions with the aluminum reactions included. The equilibrium code was run to get some idea of the species that exist during the reaction, and those that later appear after the reaction is quenched to room temperature. While these equilibrium calculations may not represent the actual gas properties, the calculations are useful as a guide to indicate which spectral lines to look for in the emission spectrum and what species to search for in the analyses of the end gas and the solid particulates.

The calculated gas properties just before reaction were given in Figure 8; gas properties after reaction are listed in Figure 16. Thirty nine species were determined to have mole fractions above 0.5×10^{-5} . In addition, 41 other species were considered in the calculations and are listed in Figure 17, but their mole fractions were less than 0.5×10^{-5} . As the reaction is quenched and the temperature reduced to 300 K, the mole fractions of the 39 most abundant species are predicted to vary in the manner shown in Figure 18. The final products are seen in Figure 18 to be mostly H₂O liquid, HCl, alumina, N₂, and ammonia, with traces of H₂O vapor.

The computed chemical equilibrium product of the NH_4ClO_4 -Al reaction were compared with the products of the .1 N_2 + .4 H_2 + .1 Cl_2 + .4 O_2 + Al reaction in order to assess how closely the shock tube conditions compare with actual rocket motor conditions. As seen in Fig. 19, both reactions have the same intermediate species in similar proportions. The use of the shock tube to simulate rocket motor conditions therefore is justified. The effect of increasing the aluminum content of an ammonium perchlorate-aluminum propellant on the resulting flame temperature was calculated using the NASA code and is shown in Fig. 20.

C. Spectrographic Results

It was initially hoped that the existence of many of the species listed in Figs. 16 and 18 could be identified from the emission spectrum of the reaction. Spectral bands or lines for many of the species have been observed in the visible and near UV and IR regions using spark discharges etc. and some of these previously observed bands are listed in Fig. 16. The spectral data was obtained from reference tables compiled by Pease¹¹, by Hertzberg¹², and by MIT Scientists¹³.

Three problems arose while measuring the emission spectrum of the aluminum reaction. First, the solid aluminum and alumina particulates gave off strong black body continuum radiation that obscured the discrete bands emitted by gaseous species¹⁴⁻¹⁷. Secondly, the AlO bands were so intense that they too obscured other bands. Thirdly, many of the minor species occur in low concentrations and have low intensity spectral bands. While the tabulated spectral data indicates the various bands that have been associated with various species, the tabulated spectral data can not predict whether or not such lines will be strong enough to be observed in any particular experiment. One would expect many of the spectral bands listed in Figure 16 to be too faint to be detectable in this experiment.

To record an emission spectrum on film, about 15 shock tube runs generally would be required. First the spectral region from 3000 - 4000 Angstroms was recorded, then 4000 - 5000 Angstroms, then 5000 - 6000 Angstroms and finally 6000 - 7000 Angstroms. For each range, three to four runs were needed to determine the proper entrance slit opening for proper film exposure. If the emission intensity was too low, several runs would be made and multiple exposures recorded. Because of the strong AlO bands, the oxygen concentration was decreased for a number of runs.

Initially, the emission spectrum of the aluminum-oxygen reaction was recorded. A typical emission spectrum is shown in Figure 21. Spectral lines associated with Al and Al⁺ are clearly visible, and four bands corresponding to AlO are seen. It was hoped that spectral bands that could be associated with Al₂O, AlO₂ or Al₂O₂ could be identified, but none were seen. The computations plotted in Figure 16 indicate that such species will be present; however no information about their spectral characteristics could be found in the literature. It is suspected that the emission spectrum emitted by these species lies in the ultra violet region that cannot be recorded using the windows and film of the present experiment. It was hoped that any weak visible bands might become strong enough to be recorded by increasing the gas temperature by using stronger shock waves, since emission intensity increases approximately as T⁴. However the strong AlO bands also became more intense and obscured a large portion of the spectrum.

The emission spectrum of the Al-N₂-H₂-O₂-Cl₂ reaction was studied next. Numerous lines and bands were observed. It is difficult to associate the bands with the various species listed in Figure 16 because many of the bands listed overlap each other. Therefore, runs were made in which various species were removed from the reactant gas mixture in a systematic way. Spectra were recorded for the Al-H₂, Al-Cl₂, AlO₂, Al-H₂-O₂, Al-Cl₂-H₂ and Al-N₂-H₂-Cl₂ reactions. A typical emission spectrum

for the $\text{Al-N}_2\text{-H}_2\text{-Cl}_2\text{-O}_2$ reaction is shown in Figure 22; the bands observed can be compared to known spectral bands, which were measured in this study using reference lamps and are shown in Figure 23. AlO , Al , Al^+ , H , N , O , O^+ , and N^+ have been positively identified. There is some evidence that observed bands belong to OH and AlH also, but the bands were too weak to be positively identified. Other weak bands could not be positively identified, but most probably were associated with AlOH , AlCl , and AlCl_2 . A strong continuum also was measured; this continuum has been reported in previous studies¹⁸ and is believed to be associated with Al_2O_2 .

D. Chemical Kinetics

Diffusion flames will typically surround burning aluminum particles and will exist near the liquid aluminum layer near the burning surface in a rocket motor. For such diffusion flames, the overall reaction process is said to be diffusion controlled since the rate of diffusion of fuel and oxidizer to the reaction zone is slower than the reaction rate determined by the chemical kinetics. However, chemical kinetics play an important role within the reaction zone itself, which is illustrated in Figure 1. The width of the reaction zone and the state of the final products depend strongly on chemical kinetics. For these reasons, the present experiment more closely simulate the reaction zone near a burning particle than say, a fast flow reactor in which the reactants are premixed and diffusive processes are ignored.

In any study of chemical kinetics, the following general steps are usually necessary, and may require many years of intensive study.

- a) The major species of interest must be identified. Methods to measure the concentration of the gaseous reactants (i.e. Al , O_2 , etc.), the products (Al_2O_3) and all intermediate

(i.e. AlO, Al₂O, AlO₂, Al₂O₂) need to be developed.

Emission spectroscopy as used in the present study is useful for identifying Al, AlO, O₂ and O, but other methods such as mass spectrometry, fluorescence or Raman scattering are needed to attempt to identify Al₂O, AlO₂ and Al₂O₂.

b) The time history of the species concentrations must be recorded. In shock tube studies with premixed gaseous reactants such as A + B → C + D, the resulting chemical kinetic rate constant (k) can be determined by:

$$\frac{d[A]}{dt} = - k \cdot [A] [B]$$

Belles and Brabbs⁸ at NASA Lewis measured the intensity of a given emission band in a single pulse shock tube in order to infer $d[A]/dt$ and use the above relation to infer k. Bauer⁹ at Cornell used the same relation but measured $d[A]/dt$ by quenching the reaction after a time Δt in a single pulse shock tube and measured $\Delta[A]$ for that time period.

c) In diffusion flame studies, the spatial profiles of the various species should be measured. For example, in the Al-O₂ flame we might expect to see the profile of Al decrease from a constant on the fuel rich side of the reaction zone to zero on the oxygen rich side. The profile of O₂ should decrease to zero on the fuel rich side of the reaction zone, with the profile of AlO reaching a peak within the reaction zone; Al₂O and AlO₂, if present, probably would peak in fuel rich and oxygen rich regions, respectively.

d) The above data allow an overall reaction mechanism to be formulated.

In the present shock tube study, Steps a) and b) were partially implemented; to fully implement a) and b) and to complete Step c), additional diagnostic techniques are required. Emission spectroscopy proved successful in identifying a number of intermediate species, but not Al_2O , AlO_2 or Al_2O_2 . Researchers have been attempting to identify these species for over 20 years and only recently have mass spectrometer measurements of Mann¹ been successful in this regard.

The time history of the AlO emission band at 4846 \AA was recorded using a polychromator and photomultiplier tubes. The background continuum at 4500 \AA also was recorded. Results are shown in Figure 24. The intensity of the AlO band peaks at 1.4 msec after ignition; at 2 msec after ignition no more AlO was observed, only background continuum. The background continuum first occurs at approximately 2 msec after ignition and exists for the entire test period of 12 msec in this case.

King¹⁸ has postulated that the background continuum observed by a number of researchers may be due to Al_2O_2 . If this is so, then the results shown in Figure 24 indicate that AlO is a precursor to Al_2O_2 , which would verify that the mechanism observed by Mann¹ at low pressures also occurs at the 40 atm test conditions of this study. However, additional spectroscopic work is needed to conclusively determine if the background truly represents the presence of Al_2O_2 .

It is felt that much information concerning the $\text{Al}-\text{O}_2$ reaction and the $\text{Al}-\text{N}_2-\text{H}_2-\text{Cl}_2-\text{O}_2$ reaction can be obtained by measuring the spatial profiles of the observed emission bands. To do so, an optical multichannel analyzer or a fiber optic sensing system is needed. To measure intermediate species concentrations, laser fluorescence diagnostics have proven useful in similar studies. For example, fluorescence technique could prove useful in helping to interpret the emission spectroscopy results since the intensity of AlO bands may partly be due to chemiluminescence and may not be an accurate measure of AlO concentration.

E. Solid and Gaseous Combustion Products

The solid and the gaseous products of combustion were collected after shock tube runs and were analyzed using the following techniques: (a) scanning electron microscope, (b) transmission electron microscope, (c) electron diffraction technique, (d) X-Ray diffraction technique and (e) infrared gas analysis. Instrumentation for methods a, b, and c were provided by the Department of Materials and Metallurgical Engineering, while that for method d was provided by the Department of Chemistry. The infrared gas analysis was done at Ford Scientific Laboratories, Dearborn, Michigan by Dr. Paul Maker.

After the aluminum sample was burned in pure oxygen in the shock tube, the white powder that formed a thin layer on the inside of the shock tube walls was collected and verified to be aluminum oxide (Al_2O_3). To collect the Al_2O_3 , a carbon block was inserted in the electrode flush to the wall. After the run, the carbon block, on which the visible Al_2O_3 powder had settled, was taken to the electron microscope laboratory. Carbon was chosen as the mounting material because it is transparent to the electron microscope. The carbon remained essentially at the wall temperature and did not take part in the reaction.

A transmission electron micrograph of the Al_2O_3 particulates is shown in Figure 25. The particles are seen to be spherical and in the size range from 0.1 to 0.6 μm . Figure 26 shows a scanning electron micrograph of the collected particulates and the results of an X-Ray diffraction analysis of the particles, which indicated that the particles were Al_2O_3 . Unburned aluminum particles easily could be differentiated from Al_2O_3 particles using the electron microscope, since the Al_2O_3 particles are nonconductors and build up a surface charge. The Al_2O_3 particles appear whiter than the Al particles and eventually go out of focus as their surface charge builds up. The X-Ray diffraction results of Figure 27 show a spike in the plot of X-Ray scattering intensity versus wavelength. The spike is observed at the

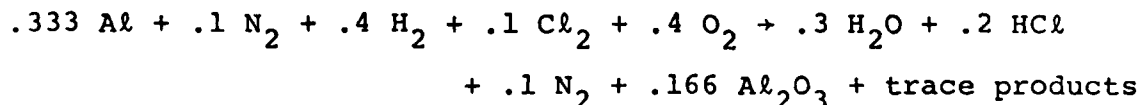
wavelength that corresponds to a pure Al_2O_3 calibration sample that was analyzed previously, indicating that the collected particles are Al_2O_3 .

When the aluminum sample was burned in the shock tube with the gas mixture $.1 \text{ N}_2 + .4 \text{ H}_2 + .1 \text{ Cl}_2 + .4 \text{ O}_2$, the products of combustion were observed to be solid particles suspended in a green colored liquid. The liquid was determined to be H_2O and HCl and the solid particles were Al_2O_3 with some unburned Al. No traces of other possible solids, such as NH_4Cl or NH_4N_3 were detected, probably because all the available hydrogen combined with the excess O_2 to form H_2O . The solid product AlCl_3 was not detected; it is deduced that the aluminum atoms combined with the excess O_2 to form Al_2O_3 rather than combine with chlorine. The result of the analysis of solid and liquid combustion products was that the only major products are Al_2O_3 , HCl and H_2O , which is consistent with results of rocket motor sampling, such as done by Strand et al.¹⁹

Various minor species were detected in the solid products of combustion. An electron micrograph of the solid products is shown in Figure 28. It is seen that the presence of condensed H_2O and HCl causes the Al_2O_3 to agglomerate into long strands, bearing no resemblance to the spherical particle from the $\text{Al}-\text{O}_2$ reaction which were shown in Figure 25. The regions that appear grey in Figure 28 are Al_2O_3 and H_2O ; the regions that appear white contain chlorine, as deduced from quantitative X-Ray analysis. The X-Ray analysis indicates elemental components only and, as seen in Figure 28, verifies the presence of aluminum and chlorine in large quantities. Trace amounts of copper, iron and silicon are detected, which were contributed by the copper electrodes, the steel diaphragm and the glass windows, respectively. A magnified view of a chlorine containing region is shown in Figure 29. It is suspected that the chlorine is in the form of HCl ; the possibility of the presence of AlCl_3 particles exists but could not be verified with the analysis techniques available.

From the above results, it is concluded that HCl and H₂O have major effects on the agglomeration of Al₂O₃. Future work in the shock tube facility would be necessary to systematically study the effects of HCl on the nucleation of Al₂O₃ and the resulting particle sizes. It is known that HCl in rocket plumes acts as nucleation sites for H₂O condensation and thereby enhances contrail visibility. The shock tube provides ideal controlled conditions for studying how chemical species affect Al₂O₃ condensation.

The results of the analysis of gaseous products of combustion for the Al-N₂-H₂-Cl₂-O₂ reaction are shown in Figure 30. An evacuated sample bag was filled with the gaseous products of combustion that remained in the shock tube after a run. The sample was analyzed at Ford Scientific Labs using infrared gas absorption analysis. The absorption bands seen in Figure 30 correspond to HCl and H₂O, the two most abundant products. Since the HCl and H₂O exist in liquid-vapor equilibrium, it was not possible to accurately measure the amount of H₂O or HCl formed, since most of it condensed on the shock tube walls. An estimate of the final H₂O and HCl concentrations could be inferred from an overall species balance:



For the shock tube run conditions, .025 moles of the test gas and .008 moles (.21 grams) of aluminum were consumed.

An unexpected result was the large fraction of nitric oxide (NO) and nitrous oxide NO₂ that was measured in the gaseous products. The NO and NO₂ bands are clearly prominent in Figure 30; the measured level of NO and NO₂ were 0.4% and 0.06% of the products. These levels are at least three orders of magnitude larger than the predicted equilibrium results, some of which are shown in Figure 18. It is believed that the unexpectedly high levels of NO and NO₂ are a result of the "prompt NO" mechanism that is well documented in hydrocarbon-air flames. In such flames

the final NO and NO_2 levels are found to greatly exceed the predicted equilibrium levels whenever the hot combustion products which contain NO and NO_2 are cooled so fast that the slow reaction that deplete NO and NO_2 do not equilibrate. Such a mechanism would explain the NO and NO_2 levels measured in the present study, which are frozen at the equilibrium level corresponding to 2700 K.

V. CONCLUSIONS

1. The chemical kinetic shock tube that was constructed provided controllable combustion of aluminum at conditions that simulate the surface of a burning aluminum particle in a rocket motor. Temperatures and pressures achievable (5000 K, 40 atm) were higher than for any previous controlled laboratory study of aluminum combustion, and were realistic of rocket motor conditions.
2. No distinct ignition temperature for aluminum was observed; small particles of aluminum ejected from the sample ignited at 2000 K while the entire sample always ignited at temperatures above 2400 K. Ignition occurred within a \pm 100 K range about the Al_2O_3 layer melting point, which is 2318 K.
3. Intermediate species detected in the $\text{Al}-\text{O}_2$ reaction by emission spectroscopy were: Al , Al^+ , and AlO . Intermediate species detected in the $\text{Al}-\text{N}_2-\text{H}_2-\text{Cl}_2-\text{O}_2$ reaction at 40 atm, 5000 K were: Al , Al^+ , AlO , H , O , O^+ , N . Weak bands that could not be conclusively identified were believed to be due to AlH , OH , AlOH and AlCl . A strong continuum was measured which has been associated with Al_2O_2 in other studies.
4. No emission bands were found that could be identified with intermediate species Al_2O or AlO_2 . Additional diagnostic techniques such as fluorescence or Raman scattering are needed to detect these species.
5. Time histories of the AlO band at 4846 \AA and the continuum at 4500 \AA indicate that the AlO emission reaches a maximum before the continuum reaches a maximum. If the continuum can be associated with Al_2O_2 , this would verify that AlO is a precursor to Al_2O_2 in the reaction mechanism.

6. Spherical Al_2O_3 particles were formed in the size range .1 - 1.0 microns when aluminum was burned in pure oxygen. When aluminum was burned in the presence of N_2 , H_2 , Cl_2 , and O_2 , extensive agglomeration of the Al_2O_3 particles was observed; the major products were Al_2O_3 , HCl and H_2O only. The solid products were analyzed using a transmission electron microscope, and X-Ray and an electron diffraction method.
7. The primary gaseous products measured were HCl and H_2O , but levels of NO and NO_2 measured were more than 10,000 times the predicted equilibrium concentrations. The unexpectedly high levels of NO and NO_2 may be due to a "prompt NO" non-equilibrium process that is observed to occur in hydrocarbon flames.

VI. RECOMMENDATIONS

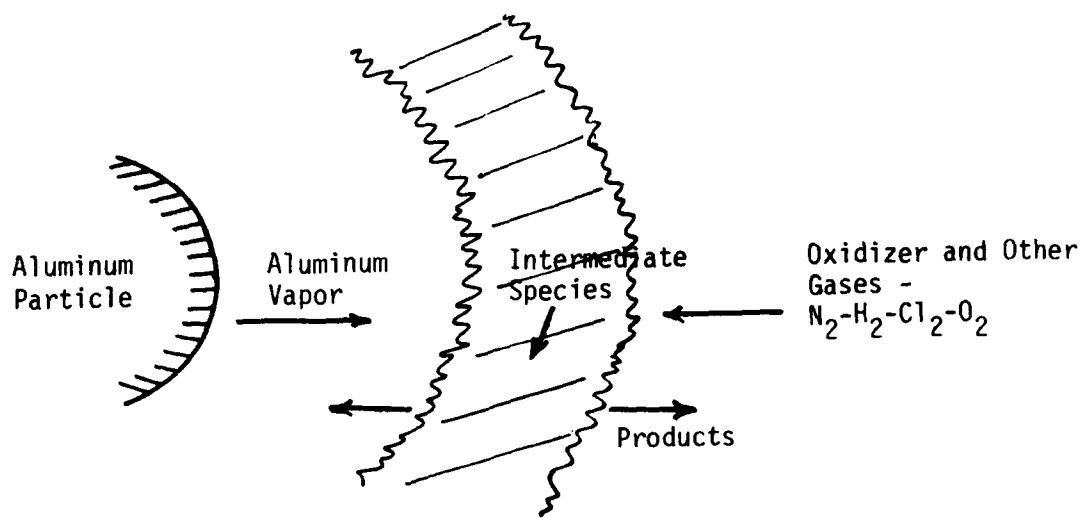
A chemical kinetic shock tube has been demonstrated to be an effective and controllable method to study metal combustion processes. However, adequate diagnostic techniques are needed to identify the numerous chemical species present. To provide new contributions to the understanding of the reaction mechanism and the condensation/agglomeration process, the following is recommended.

1. Add fluorescence and Raman diagnostics to the emission spectroscopy techniques used in the present study.
2. Measure the spacial profile of AlO, Al, O₂ through the reaction zone, which requires a set of diode arrays or an optical multichannel analyzer (OMA) to scan various locations simultaneously.
3. Assess the effect of HCl and chemical additives on the size distribution of Al₂O₃ particles formed; this can be carefully controlled in a shock tube study.
4. To more closely simulate rocket nozzle condensation/agglomeration processes, the combustion products in the shock tube could be expanded through a converging-diverging nozzle. The effects of the expansion could be determined by collecting particles at various locations and comparing size distributions.

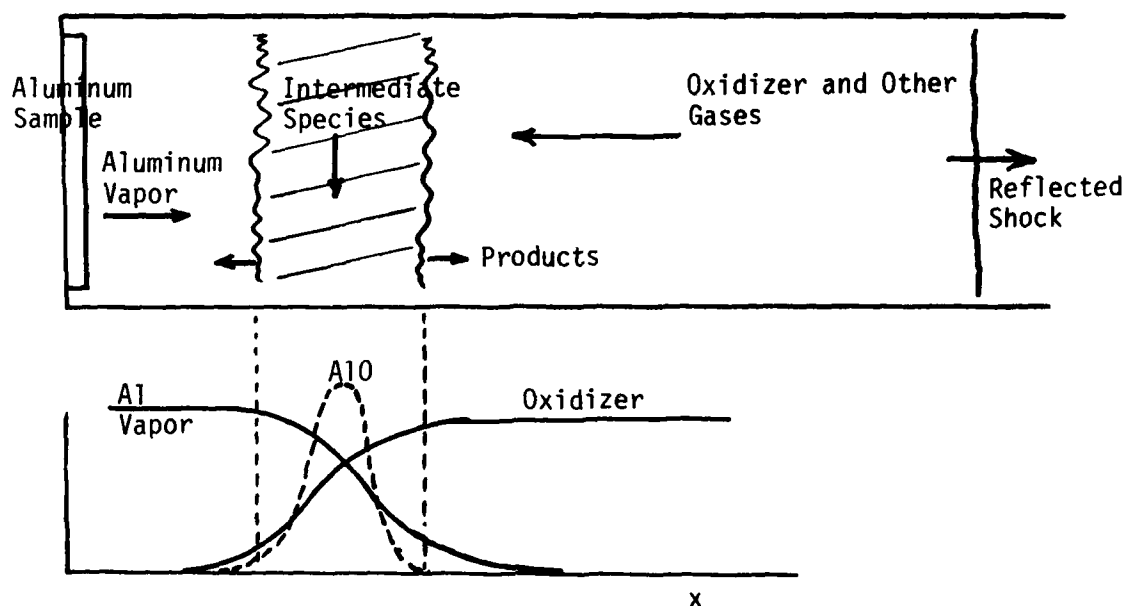
VII. REFERENCES

1. Mann, D.M., "Particulate Formation in Aluminum/Oxygen Flames," 15th JANNAF Combustion Meeting, Newport, R.I., February 1979.
2. Friedman, R. and Macek, A., "Ignition and Combustion of Aluminum Particles in Hot Ambient Gases," 9th Symposium (Int'l) on Combustion, 1963, p. 703.
3. Bourianes, R., "Combustion of Aluminum in CO₂ and O₂ Atmospheres," Comb. Flame 31, 89, 1978.
4. Prentice, J.L., "Combustion of Pulse Heated Particles of Aluminum and Be," Comb. Sci. Tech. 1, 385, 1970.
5. Henderson, C.B., "Proposed Combustion Scheme For the Gaseous Oxidation Reactions of Be and Al," Comb. Sci. Tech. 1, 275, 1970.
6. Mellor, A.M. and Glassman, I., "Augmented Ignition Efficiency for Aluminum," Comb. Sci. Tech. 1, 437, 1970.
7. Guirao, C. and Williams, F.A., "A Model for AP Deflagration Between 20 and 100 Atm," AIAA J. 9, 7, 1971.
8. Belles, F.E. and Brabbs, T.A., "Effects of Turbulent Boundary Layers on Chemical Kinetic Measurements in a Shock Tube," 9th Symposium (Int'l) on Combustion, 1963.
9. Lifshitz, A. and Bauer, S.H., "Studies with a Single Pulse Shock Tube," J. Chem. Phys. 38, 9, 1963.
10. Bernstein, L., "Tabulated Solutions of the Equilibrium Gas Properties Behind Incident and Reflected Shock Waves," Ph.D. Thesis, Univ. London, 1963.
11. Pearse, R. and Gaydon, A.G., The Identification of Molecular Spectra, Chapman and Hall, London, 1963.
12. Herzberg, G., Molecular Spectra, Van Nostrand, NY, 1950.
13. Harrison, G.R., MIT Wavelength Tables, MIT Press, Cambridge, MA, 1939.
14. Rautenberg, T.H. and Johnson, P.D., "Light Production in the Al-O₂ Reaction," J. Opt. Soc. 50, 6, 1960.
15. Edse, R., Rao, K., Strauss, W., and Mickelson, M., "Emission Spectra Excited in Metal Powder Oxygen Flames," J. Opt. Soc. 53, 4, 1964.

16. Zhdanova, L.V., "Rotational Structure of the Aluminum Oxidation Spectrum," Air Force FTD-HT-23-569-74, 1973.
17. Brzustowski, T.A. and Glassman, I., "Spectroscopic Investigation of Metal Combustion," Vol. 15, Prog. in Aero. and Astro. Heterog. Comb., 1964.
18. King, M., Atlantic Research Co., private communication.
19. Strand,L.,et.al., Characterization of Particulates in the Exhaust Plume of Large Solid-Propellant Rockets, J. Spacecraft, 18,4,1981.



(a)



(b)

Figure 1. Schematic of the Reaction Zone Near (a) An Aluminum Particle in a Rocket Motor and (b) An Aluminum Sample in a Shock Tube

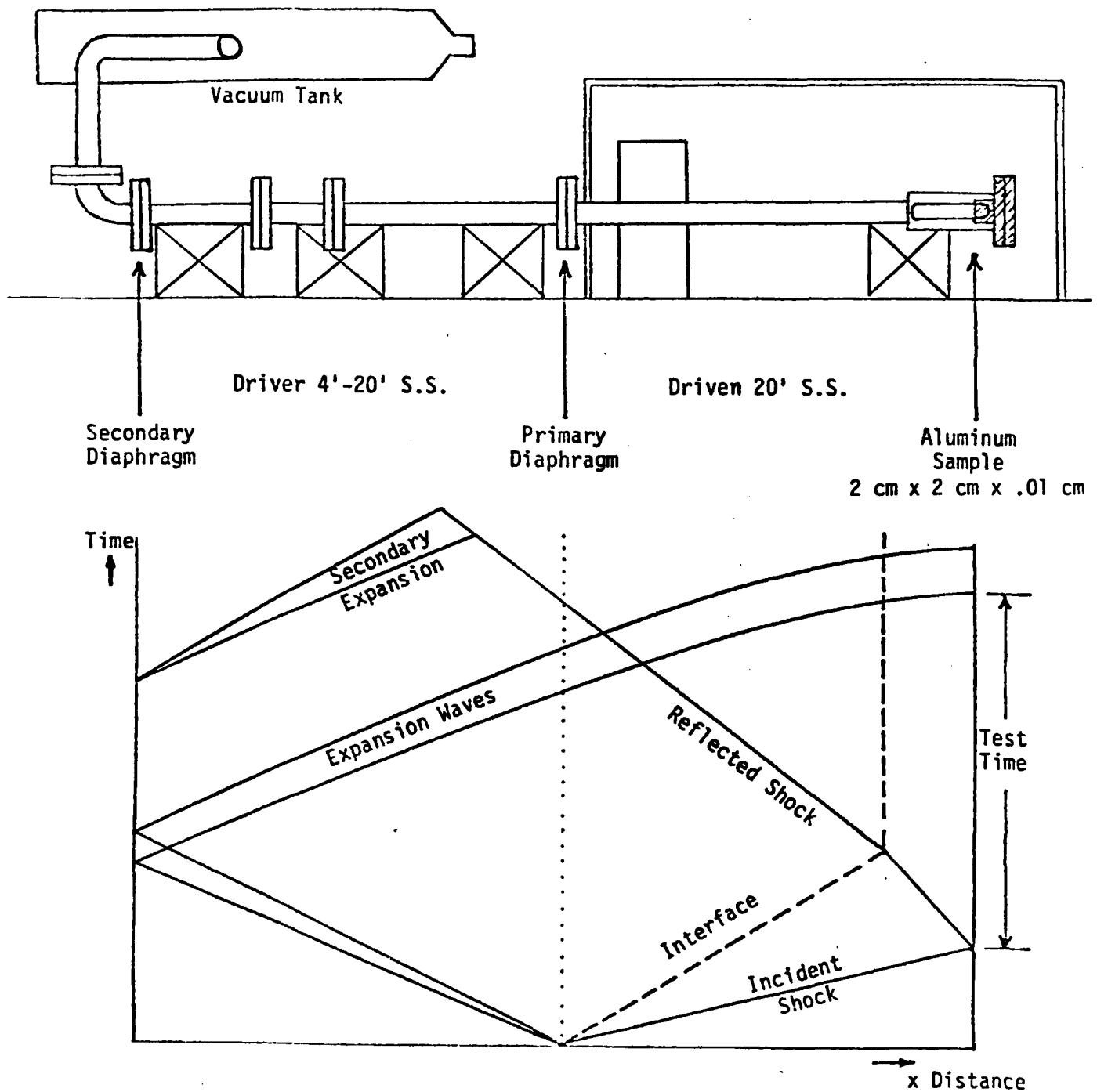


Figure 2. Schematic of Chemical Kinetic Shock Tube

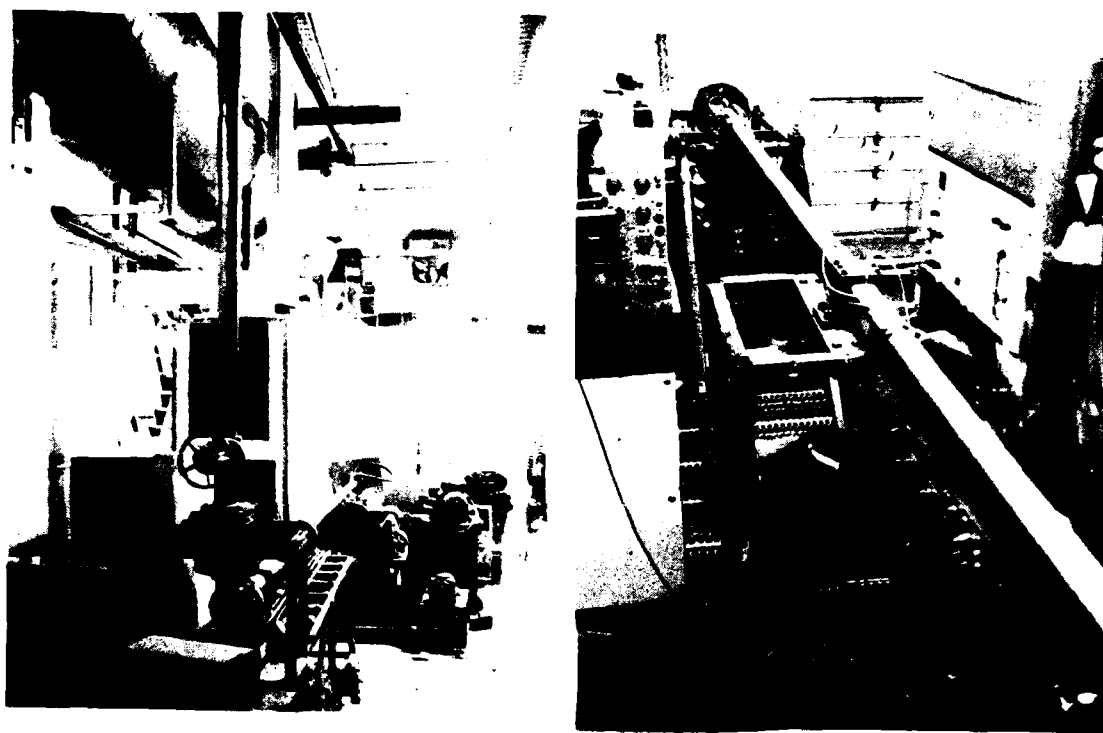
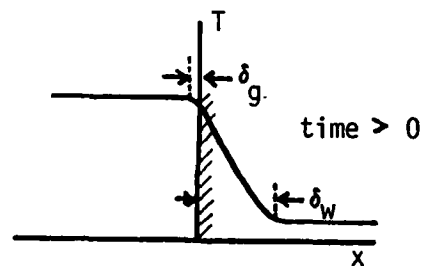
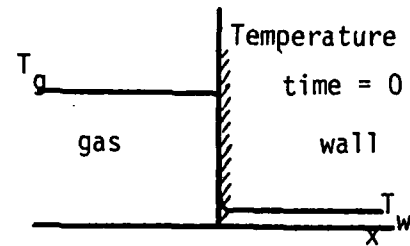
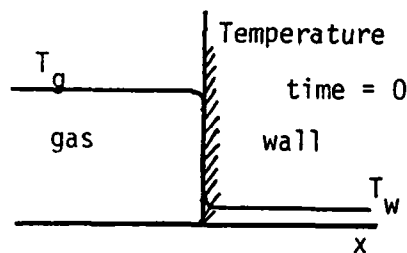


Figure 3. Photographs of Shock Tube

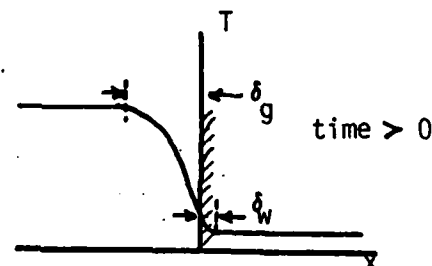
In general:

$$\frac{k_g \cdot \Delta T_g}{\delta_g} = \frac{k_w \cdot \Delta T_w}{\delta_w} ; \quad \delta_g = \sqrt{a_g t} ; \quad \delta_w = \sqrt{a_w t}$$



Case (a) wall = good insulator

$$T_{\text{sample}} \approx T_g$$



Case (b) wall = good conductor

$$T_{\text{sample}} \approx T_w$$

Figure 4. Schematic of Thermal Boundary Layer Near Sample Mounted On Shock Tube End Wall

Typical Run Conditions for Al-O₂ Reaction

Conditions behind reflected shock: 4000 K, 17 atm
Incident shock: M = 5
Initial oxygen pressure: 1.16 psi
Driver pressure: 460 psi helium

Typical Run Conditions for Al + .1 N₂ + .1 Cl₂ + .4 H₂ + .4 O₂ Reaction

Conditions behind reflected shock: 4149 K, 14.3 atm
Incident shock: M = 7.8
Initial gas pressure: .386 psi
Driver gas pressure: 400 psi helium
Molecular weight of mixture: 25.67 g/mole
Ratio of specific heats: 1.1179

Gas Composition Prior to Aluminum Ignition (Mole Fraction)

	Percent		Percent
O	17.405	Cl	9.847
OH	14.249	HCl	7.036
H	13.397	N ₂	7.008
O ₂	11.400	H ₂	6.208
H ₂ O	10.392	NO	2.936

Maximum P, T Run Conditions for Al + .1 N₂ + .1 Cl₂ + .4 H₂ + .4 O₂

Conditions behind reflected shock: 5150 K, 40 atm
Incident shock: M = 10.5
Initial gas pressure: .386 psi
Driver gas pressure: 1500 psi

Figure 5. Typical Shock Tube Operating Conditions

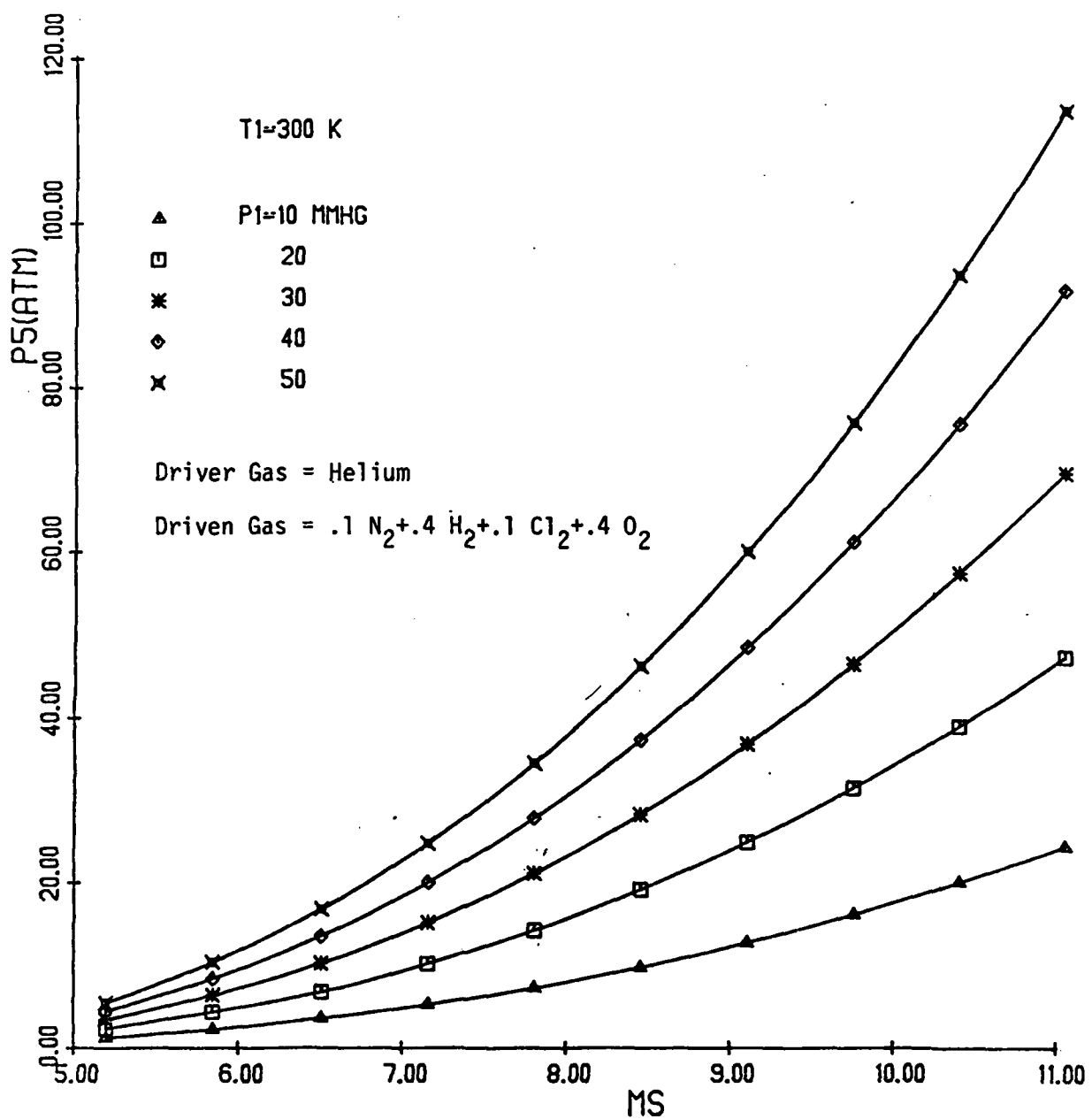


Figure 6. Gas Pressure (P₅) Behind Reflected Shock Just Prior to Sample Ignition vs. Incident Shock Mach Number; Real Gas Effects Included in Gordon-McBride Program

DRIVER GAS : HE
DRIVEN GAS : $4H_2 + 4O_2 + N_2 + Cl_2$

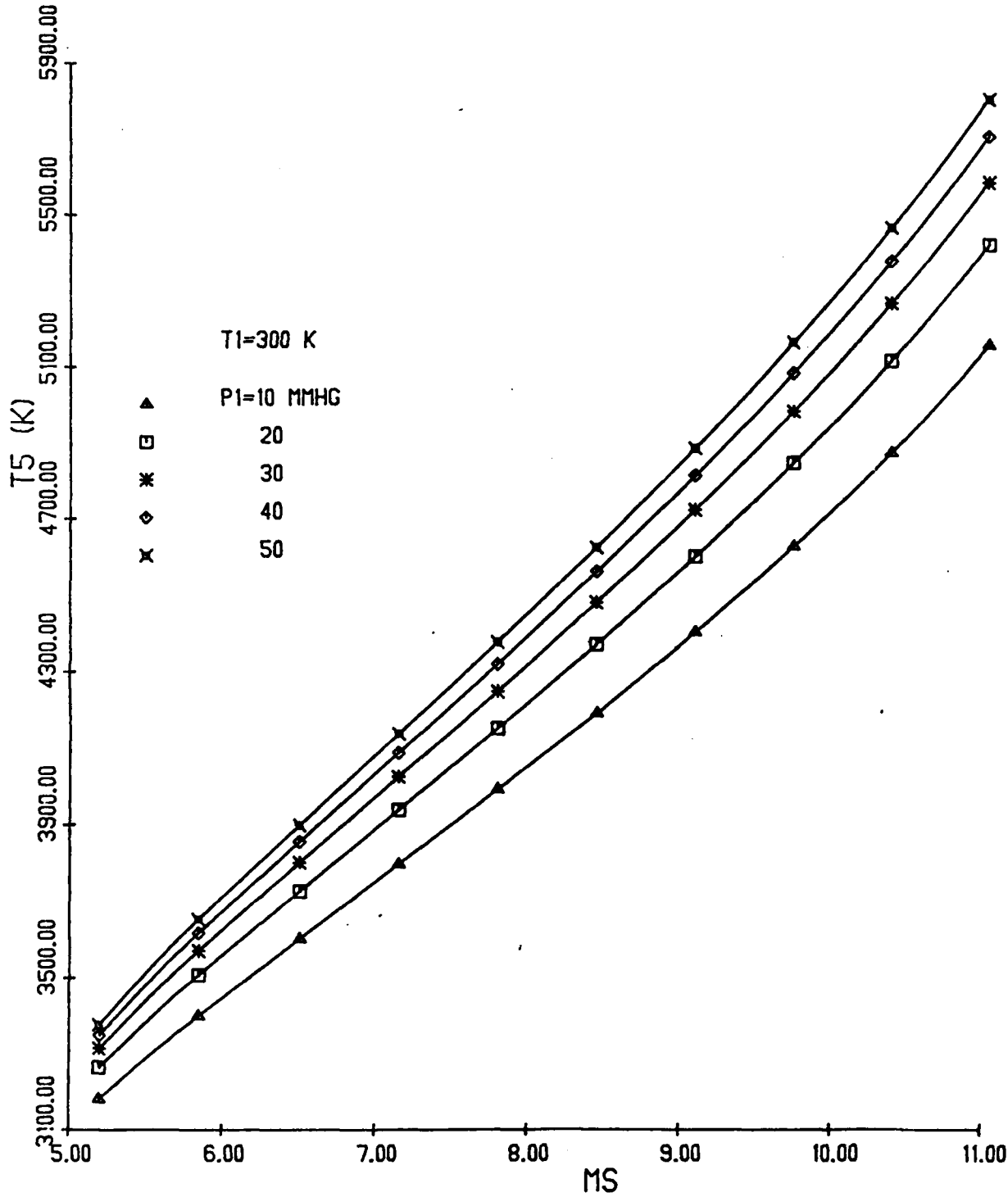


Figure 7. Gas Temperature (T_5) Behind Reflected Shock Just Prior to Sample Ignition vs. Incident Shock Mach Number (MS); Real Gas Effects Included in Gordon-McBride Program

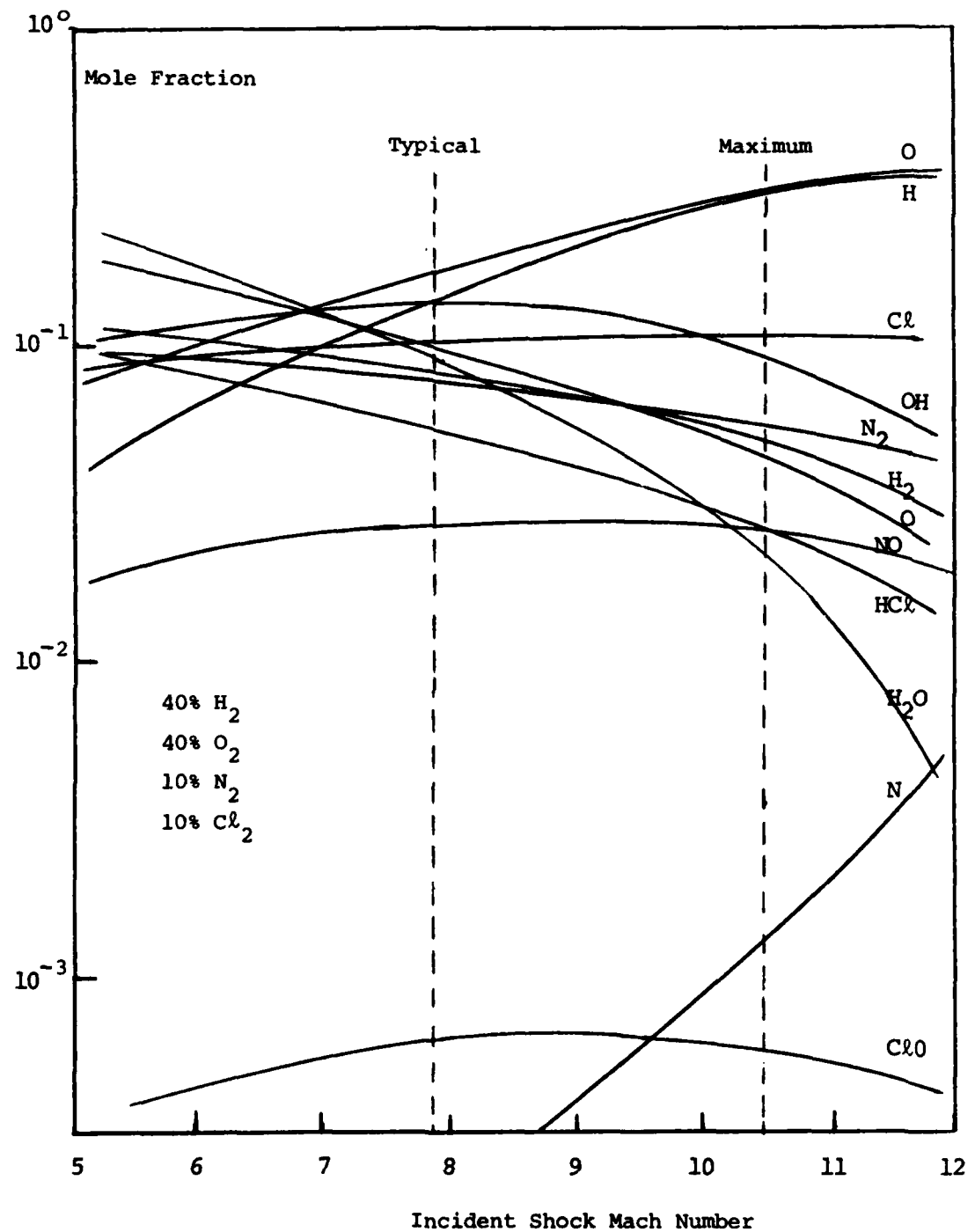


Figure 8. Composition of the gas behind the reflected shock just prior to sample ignition, real gas effects included.

DRIVER GAS : HE
DRIVEN GAS : $4H_2 + 4O_2 + N_2 + Cl_2$

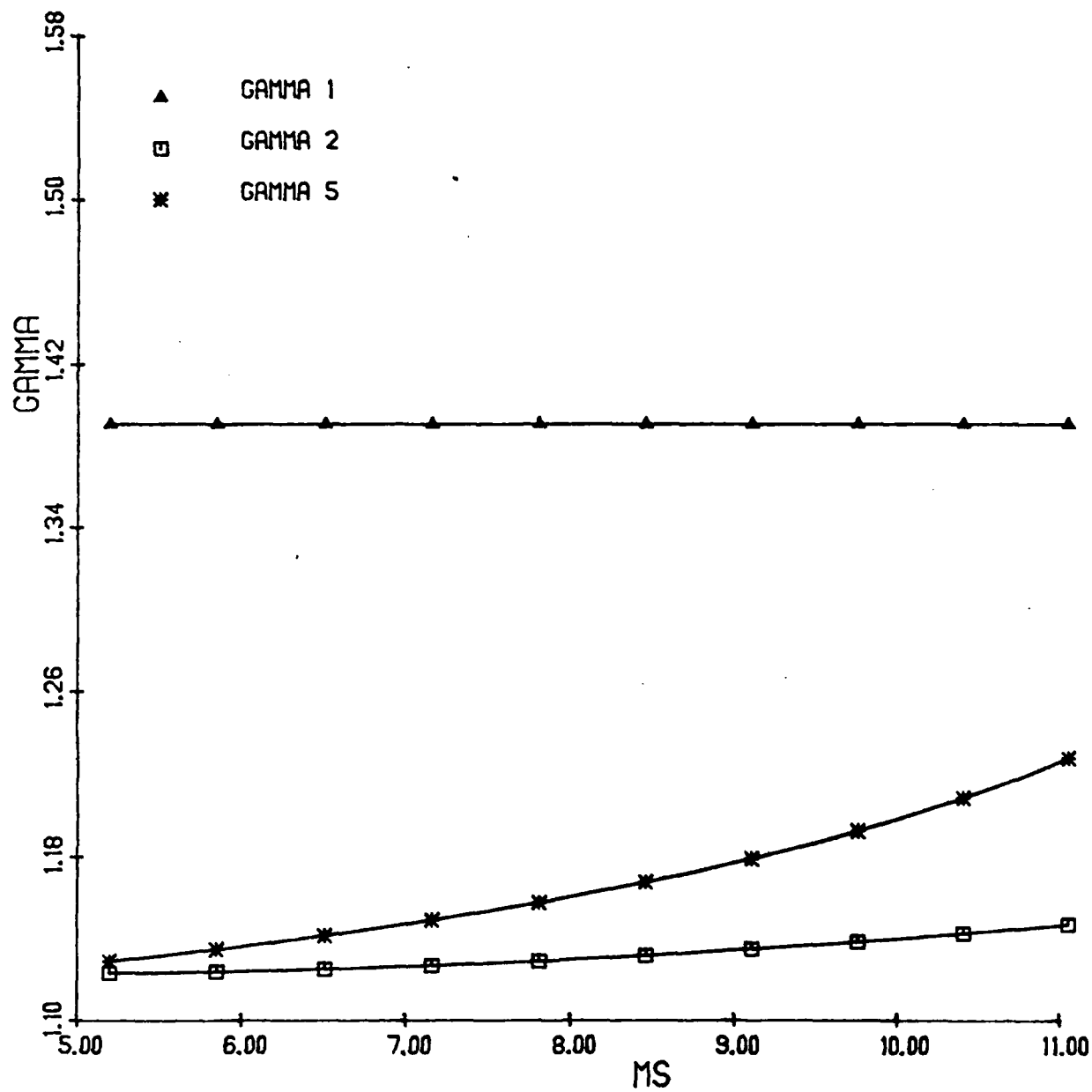


Figure 9a. Ratio of Specific Heats (Gamma) Just Prior to Ignition

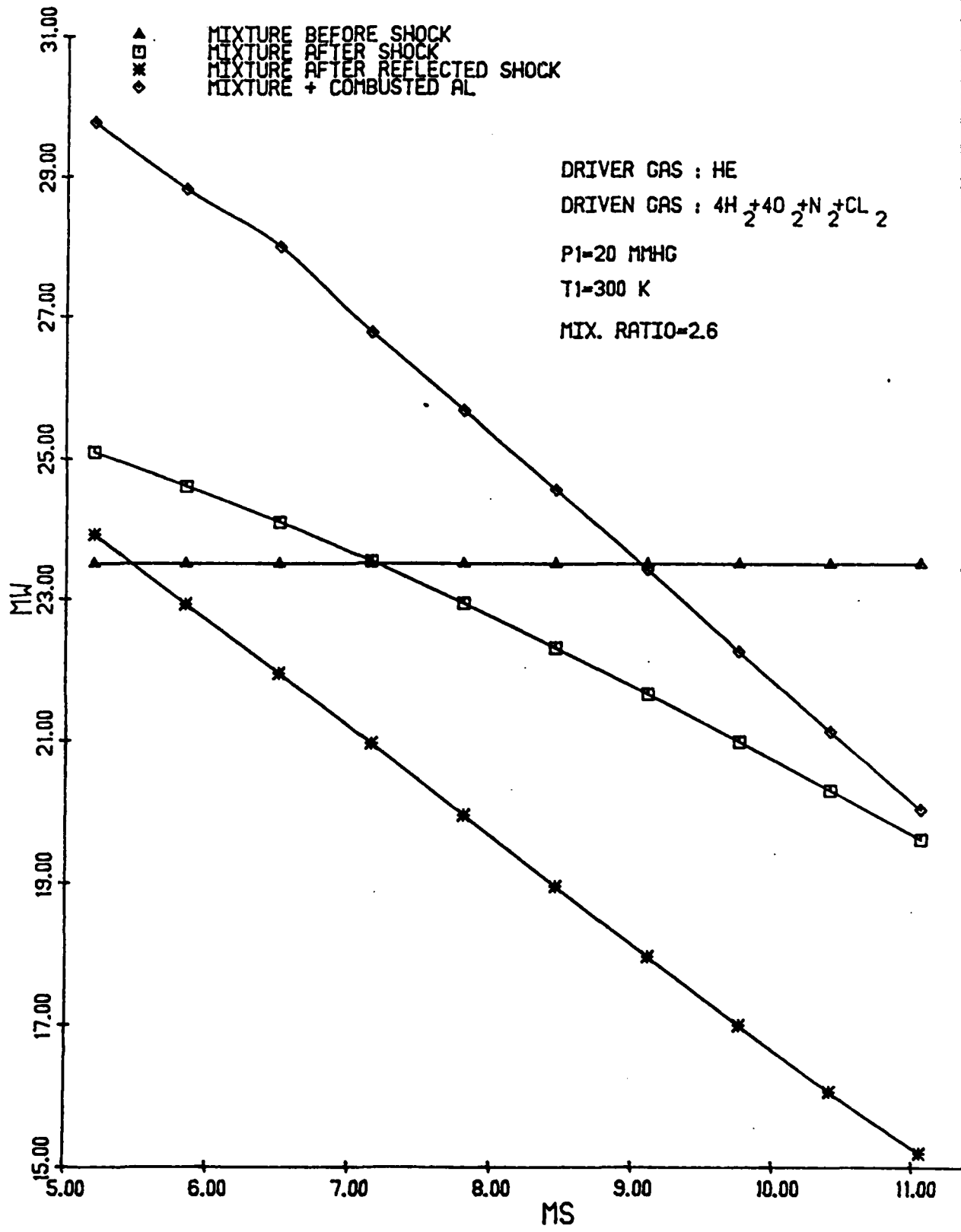


Figure 9b. Molecular Weight of Gas Prior to Ignition

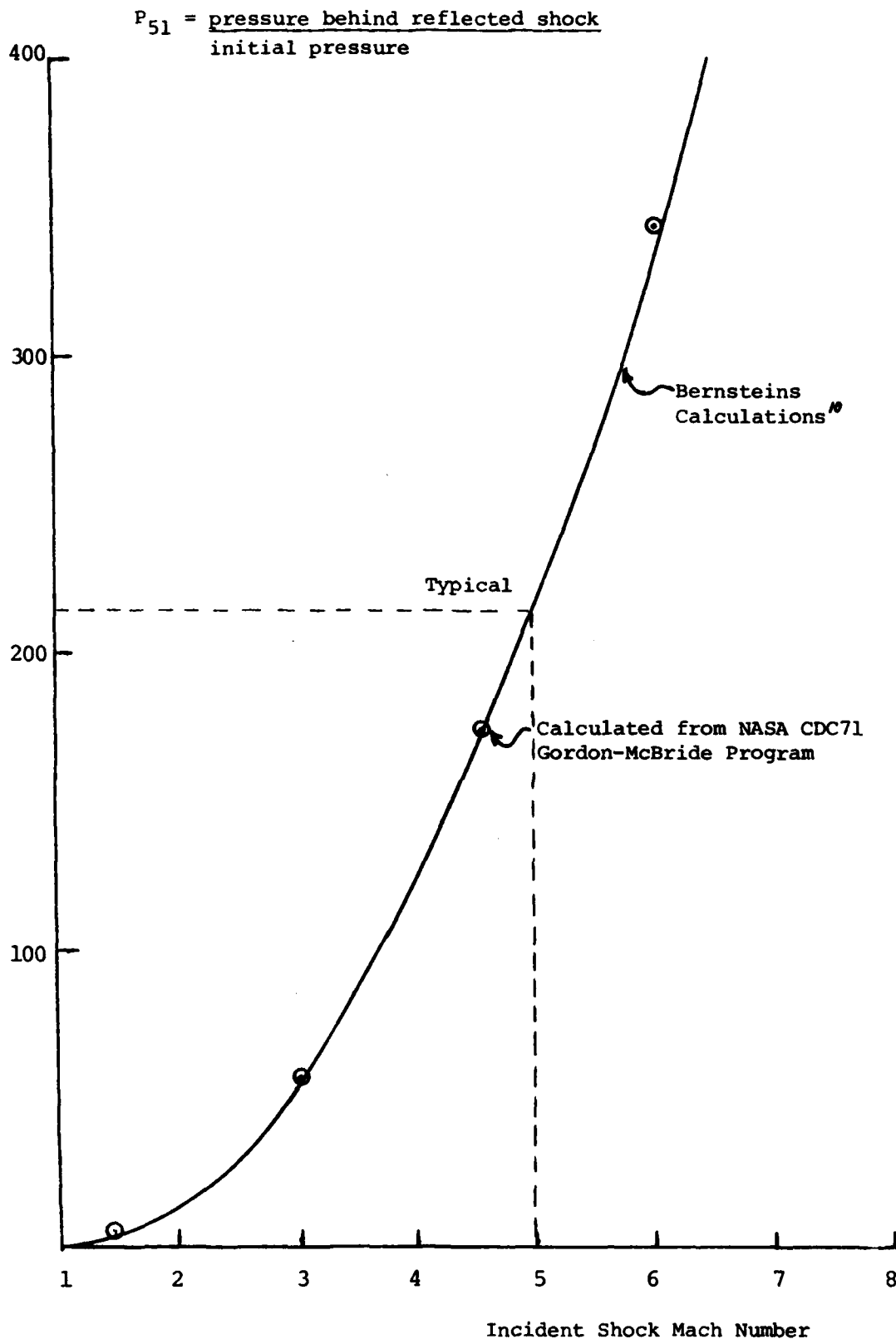


Figure 10. Run condition for pure oxygen — NASA CEC program checked for proper convergence.

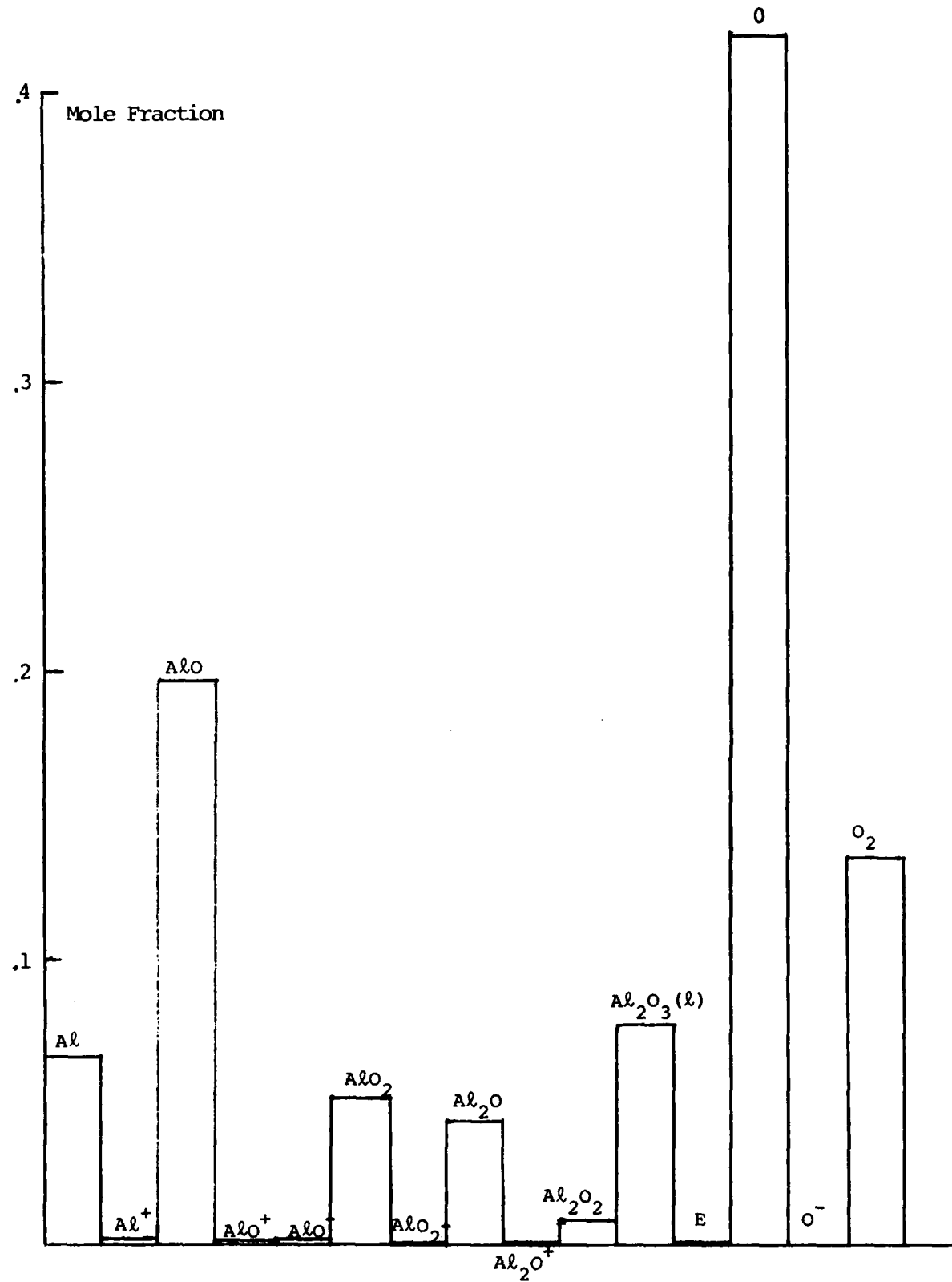


Figure 11. Equilibrium Concentrations of Species for $\text{Al} - \text{O}_2$ Reaction:
 Incident Shock Mach Number = 9.125, T_5 before Ignition = 4418K,
 after ignition = 4930K, P_5 = 28.6 atm.

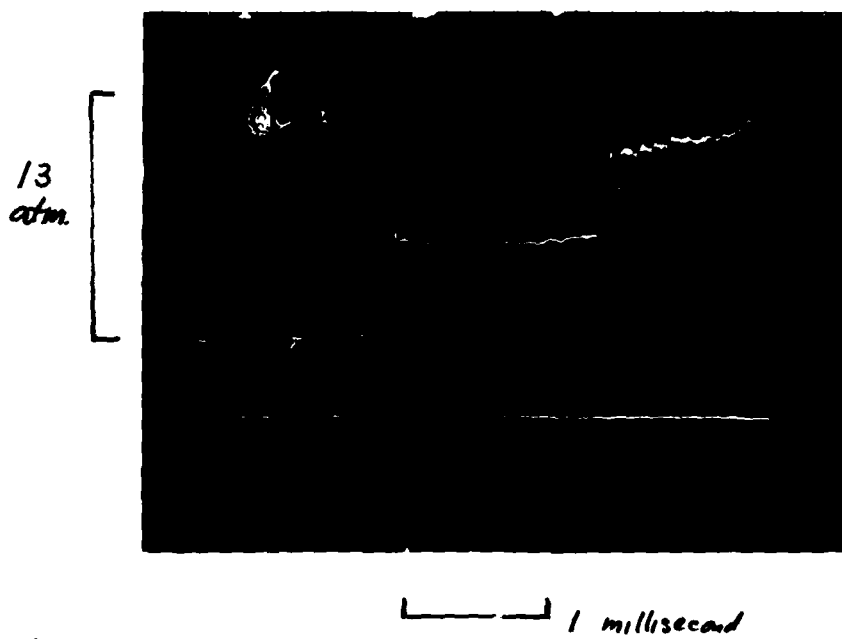
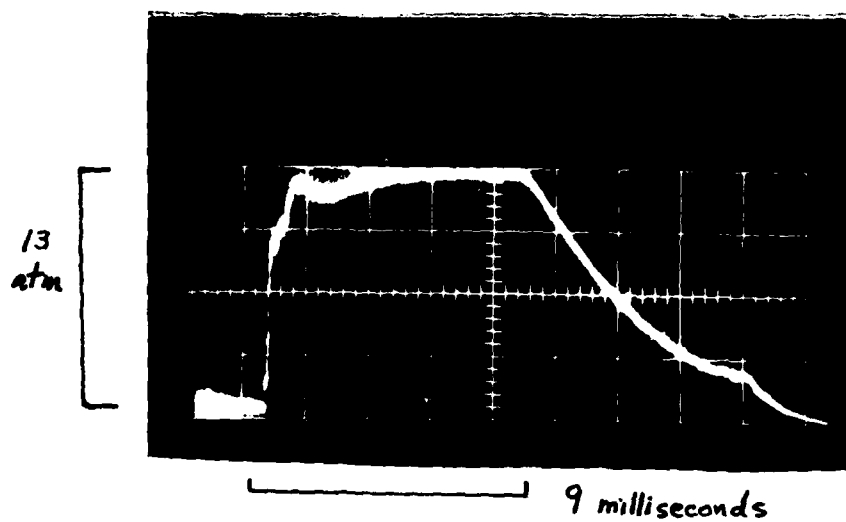


Figure 12. Oscilloscope traces showing (a) pressure history at end wall; (b) pressure history two meters from end wall.

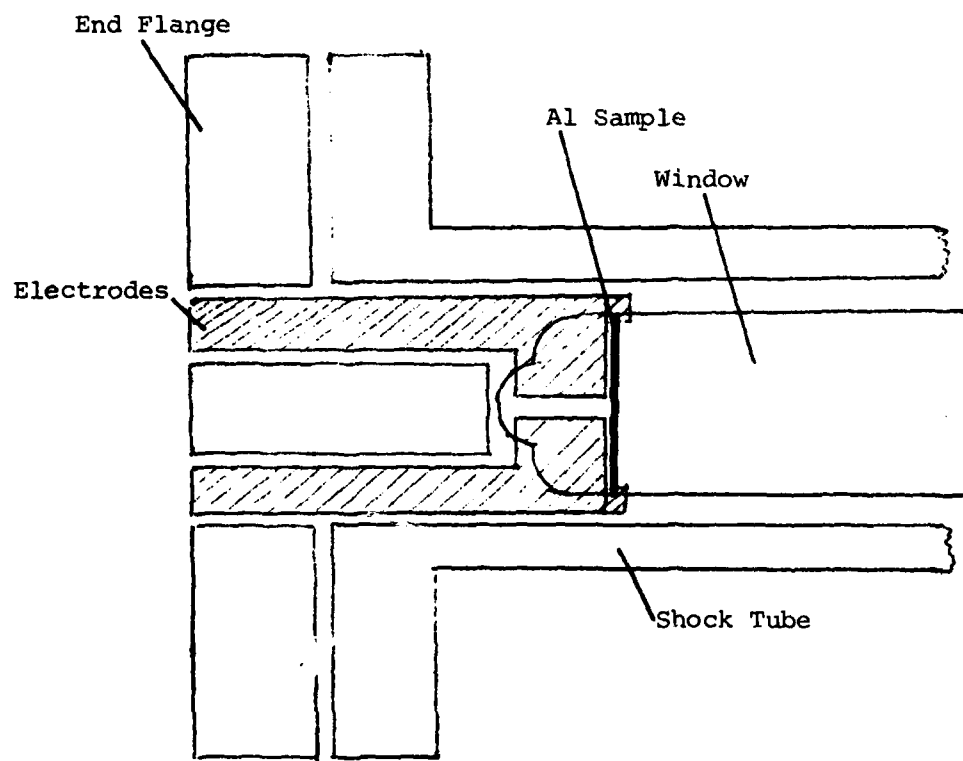
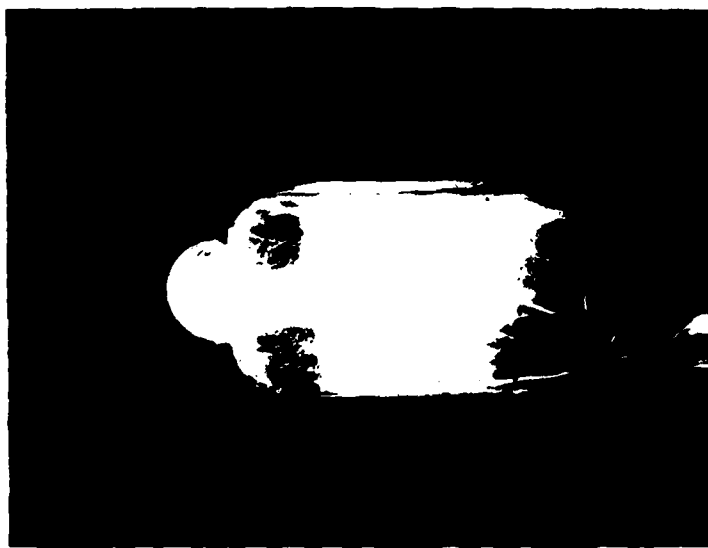


Figure 13. Photograph of the ignition of the aluminum sample mounted on shock tube end wall.



Figure 14. High speed movie of the aluminum sample ignition process.

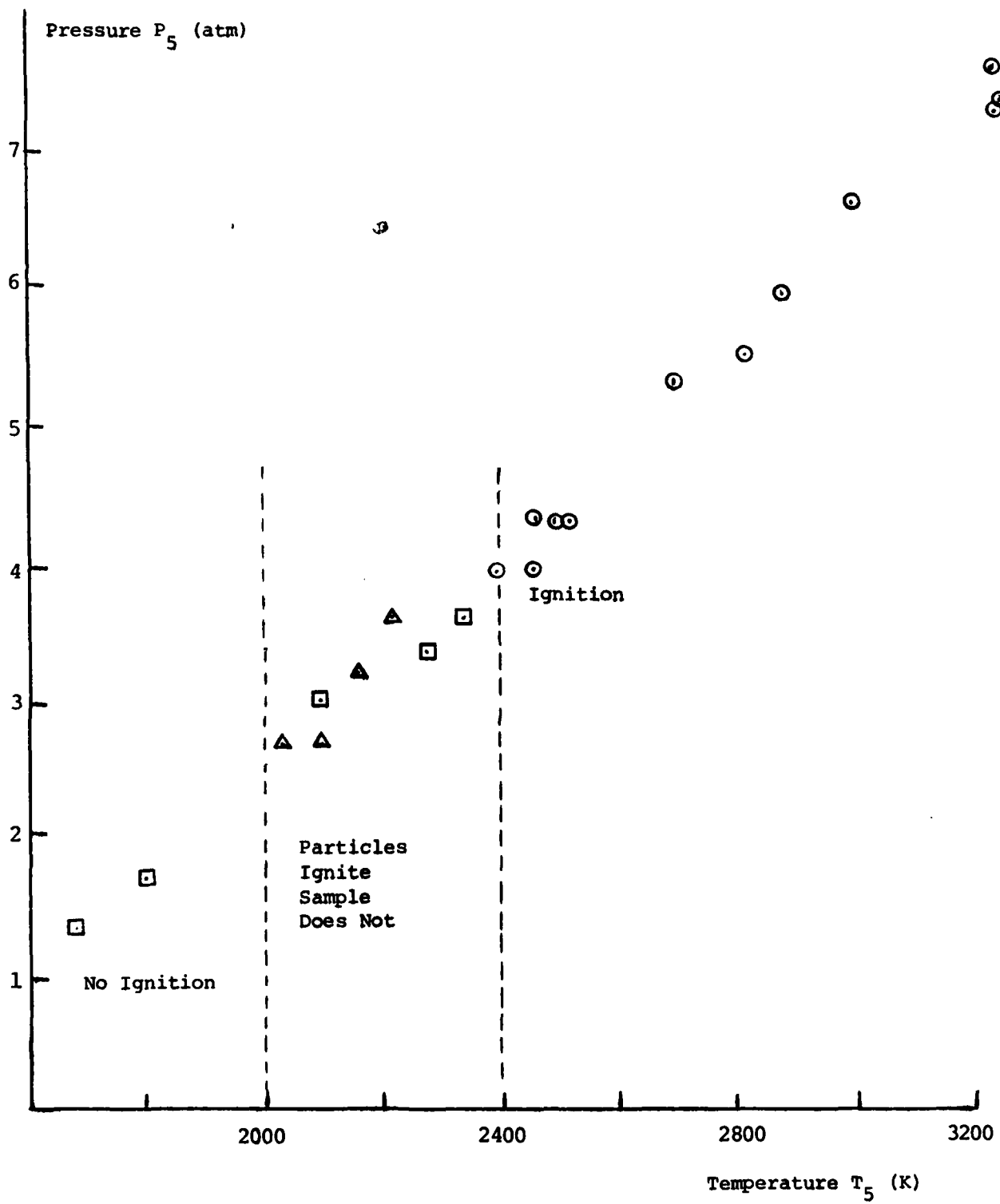


Figure 15. Aluminum ignition data for various pressure and temperatures in oxygen. \circ Ignition observed, \square No ignition observed, Δ Particles only ignite.

Species	Mole Fraction at 4360 K	Spectral Bands/Line (Angstroms)
Al	.03362	3961, 3944
Al^+	.00052	5388, 5861
AlCl_i	.03956	2555, 2708, 3972, 4154, 5265, 5612
AlCl_2	.00134	
AlH	.00085	2700, 3380, 3800, 4752, 4354, 2033, 2229, 4241, 4259
AlO	.05226	4648, 4842, 5079, 5336
AlOCl	.01475	
AlOH	.00639	
AlO_2^-	.01486	
AlO_2^-	.00030	
AlO_2H	.01139	
Al_2O	.00647	
Al_2O_2	.00022	
$\text{Al}_2\text{O}_3 (\lambda)$.03308	
Cl	.05977	4810, 4819, 4794
Cl^-	.00022	
ClO	.00028	3623
Cl_2	.0002	5510, 4817, 4864
H	.20344	6562, 4861, 4340, 4101
HCl	.03519	7463, 9152, 3.5 μm
HNO	.00001	7341, 7718, 6715, 7061
H_2	.07724	6000, 4615
H_2O	.05205	2.5 μm , 3.5 μm , 9420, 9060, 8227, 7957, 7227, 6994, 6524, 6324, 5952, 5924, 5722

Figure 16. Calculated Mole Fractions of Various Species in the $\text{Al}-\text{O}_2-\text{N}_2-\text{Cl}_2-\text{H}_2$ Reaction at 4360 K. Also listed are spectral lines/bands that are known to be associated with each species. Continued.

<u>Species</u>	<u>Mole Fraction at 4360 K</u>	<u>Spectral Bands/Line (Angstroms)</u>
N	.00040	5676, 4109, 4099, 5679, 5666, 4103, 4097
NH	.00002	3240, 3360, 4502
NH ₂	.00001	6302, 5977, 5708, 5166, 5436
NO	.01838	3008, 2859, 2722, 2595
NO ₂	.00001	2491, 2459, 4480, 4630, 4448
N ₂	.06689	4666, 4344, 4059, 3805, 3577, 3371
O	.13922	6158, 5330, 4368, 3947
OH	.09435	3064, 3100
O ₂	.03660	2221, 3671, 3914, 4179, 4880, 4577, 4309, 3370

Figure 16. continued

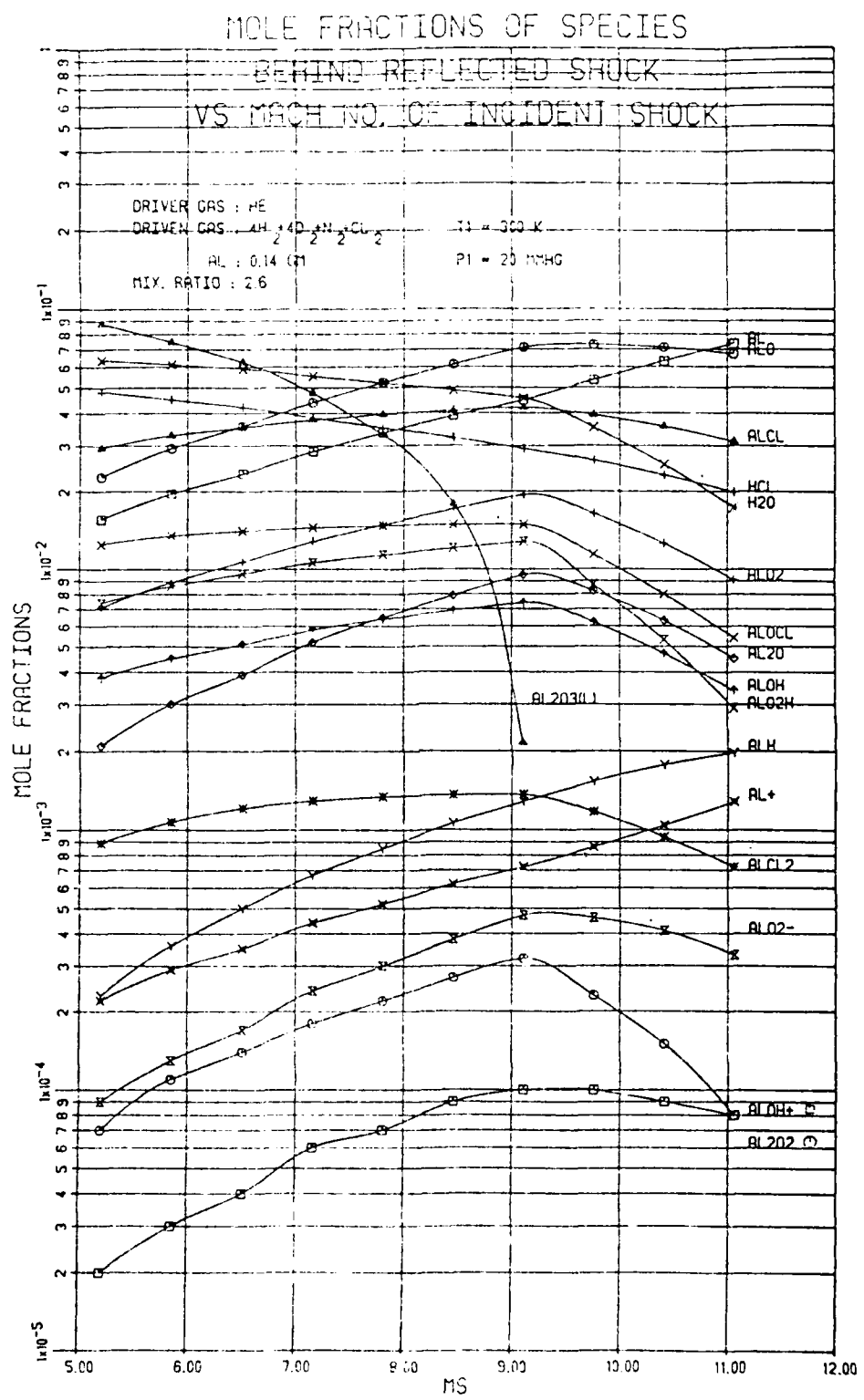


Figure 16. continued

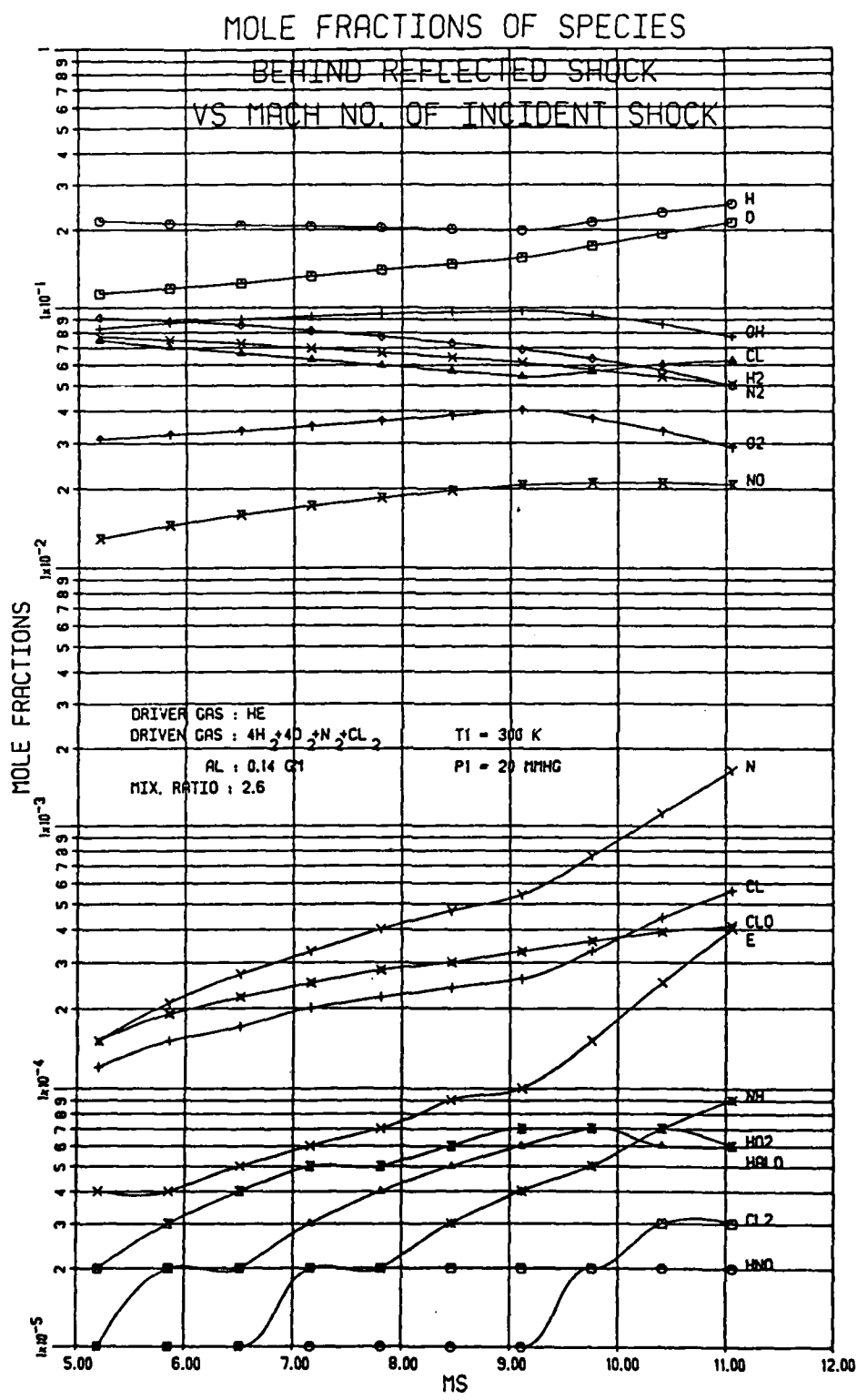


Figure 16. concluded

Al(S)	Cl^+	NH_3
Al(l)	ClO_2	NO^+
AlCl^+	Cl_2O	NOCl
AlCl_2^+	H^+	NO_2^-
AlCl_2^-	H^-	NO_2Cl
$\text{AlCl}_3(\text{S})$	HNO_2	NO_3
$\text{AlCl}_3(\text{l})$	HNO_3	N_2H_4
AlN(S)	$\text{H}_2\text{O(S)}$	N_2O
AlN	$\text{H}_2\text{O(l)}$	N_2O^+
AlO^+	H_2O_2	N_2O_4
AlOH^-		N_2O_5
Al_2Cl_6		N_3
Al_2O_2^+		O^+
$\text{Al}_2\text{O}_3(\text{S})$		OH^+
		OH^-
		O_2^-
		O_3

Figure 17. Other Species Considered in the Calculations Whose Mole Fractions Were Less Than 5×10^{-6} .

MOLE FRACTIONS OF CONDENSED SPECIES

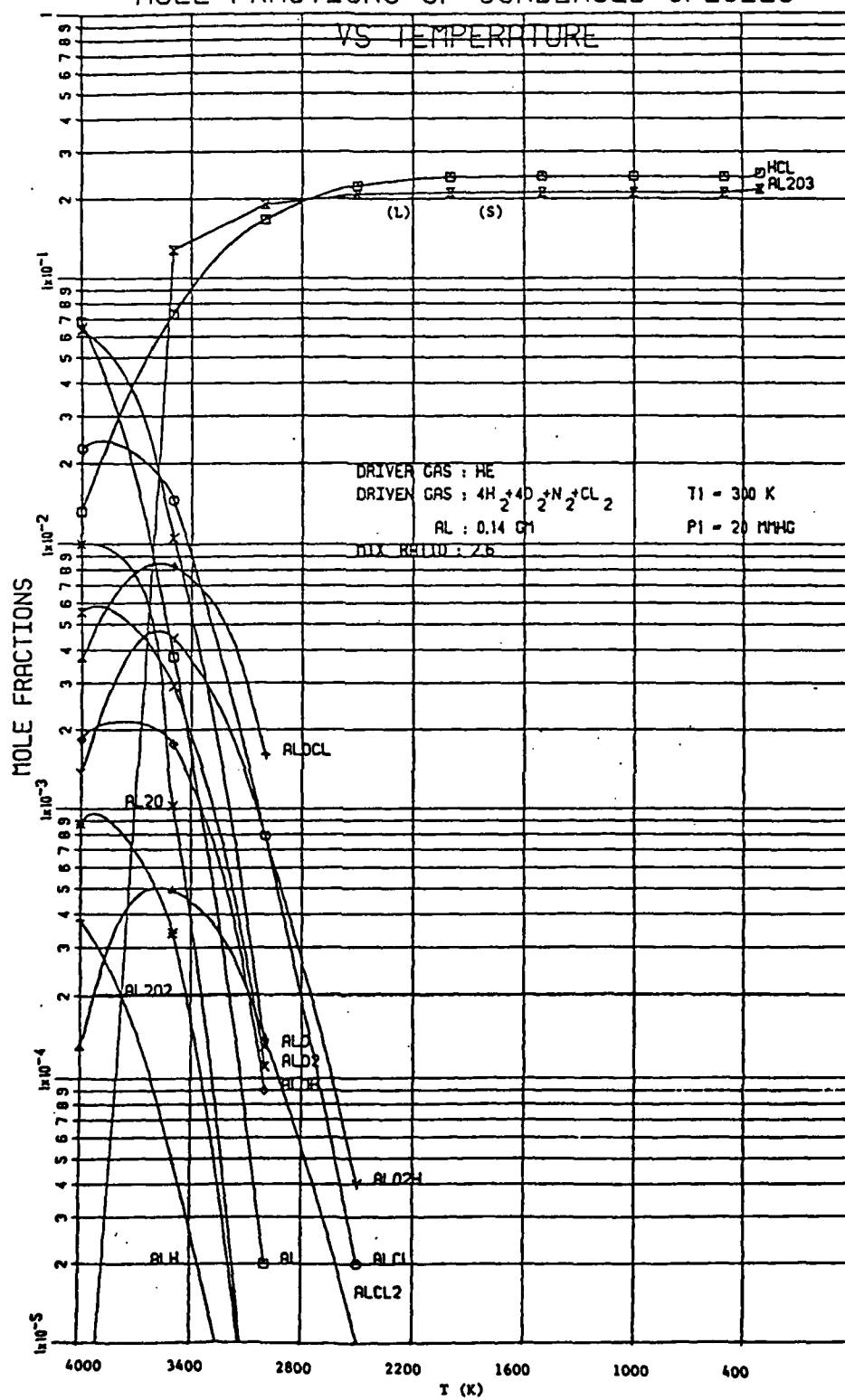


Figure 18. Variation of Reaction Products as Temperature Decreases to 300 K

MOLE FRACTIONS OF CONDENSED SPECIES

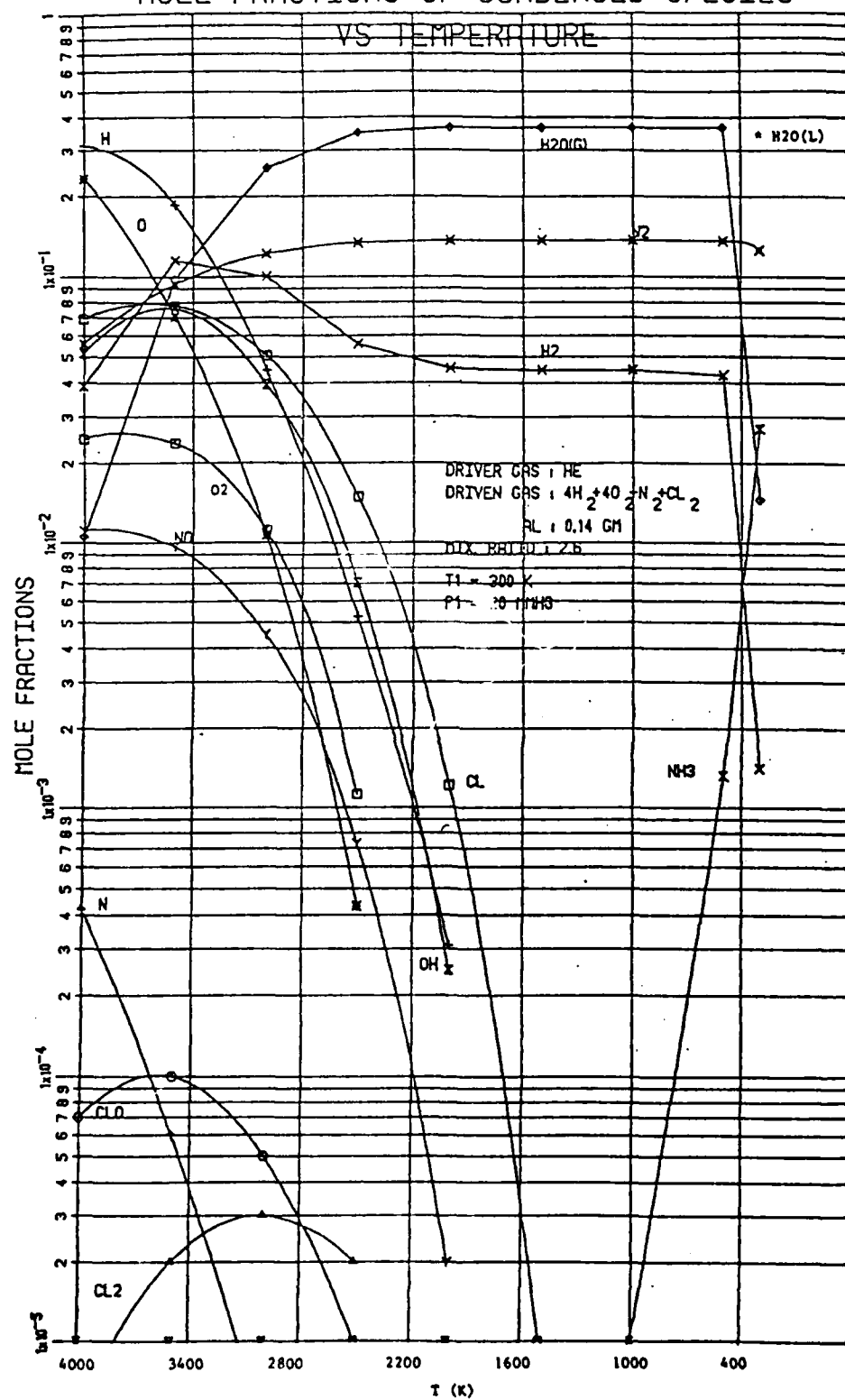


Figure 18. concluded

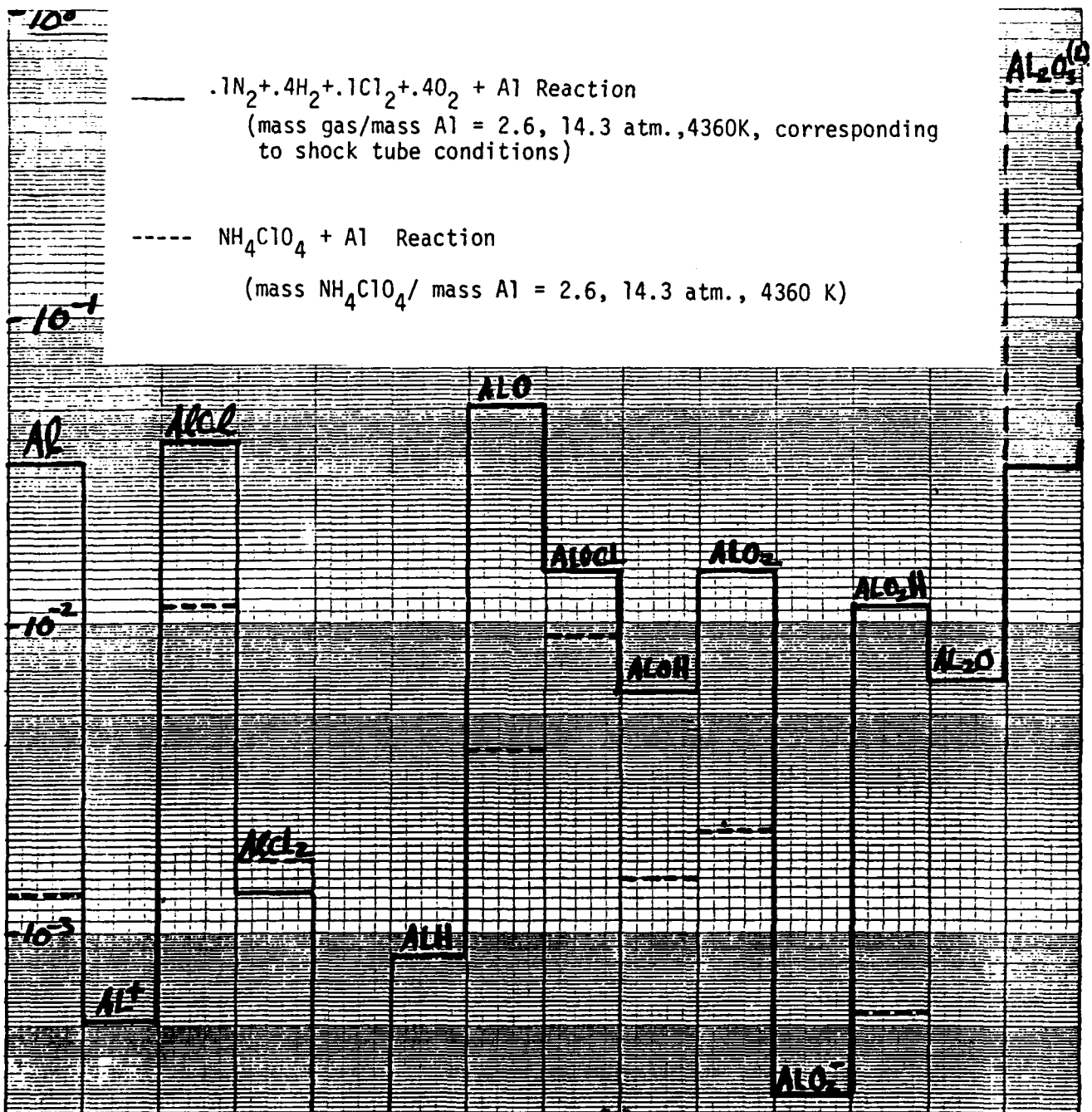


Figure 19. Comparison of Computed Equilibrium Products of the $\text{NH}_4\text{ClO}_4 - \text{Al}$ Reaction with those for the $\cdot 1\text{N}_2 + .4\text{H}_2 + .1\text{Cl}_2 + .4\text{O}_2$ Reaction

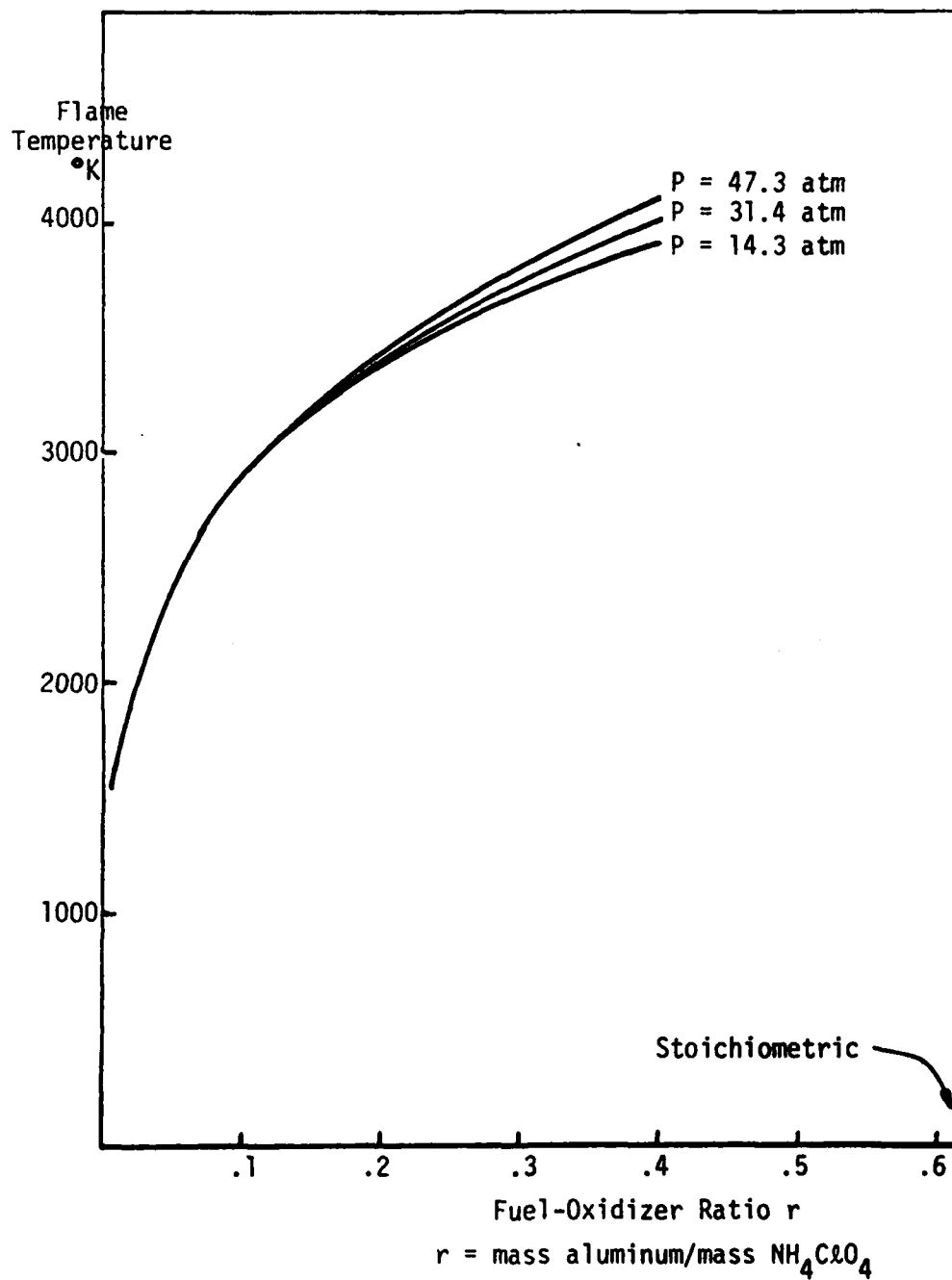
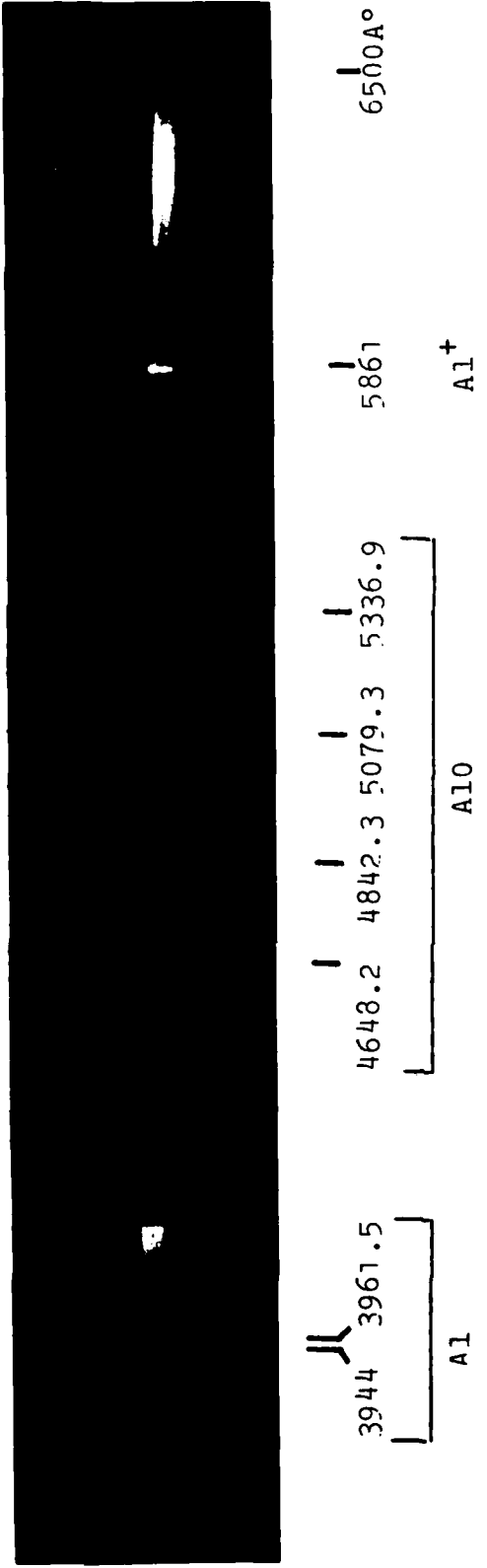


Figure 20. Aluminum- NH_4ClO_4 Flame Temperatures Calculated Using NASA Equilibrium Code



Conditions Behind Reflected Shock:

$$P_5 = 7.1 \text{ atm}$$

$$T_5 = 2700 \text{ K}$$

Exposure time = 8 msec

Figure 21. Emission spectrum of aluminum - oxygen reaction in the shock tube

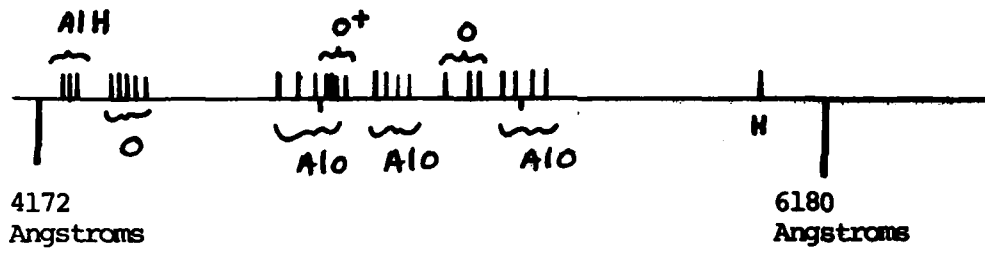


Figure 22. Schematic of Emission Spectrum Observed For
The $\text{Al}-\text{H}_2-\text{O}_2-\text{Cl}_2-\text{N}_2$ Reaction

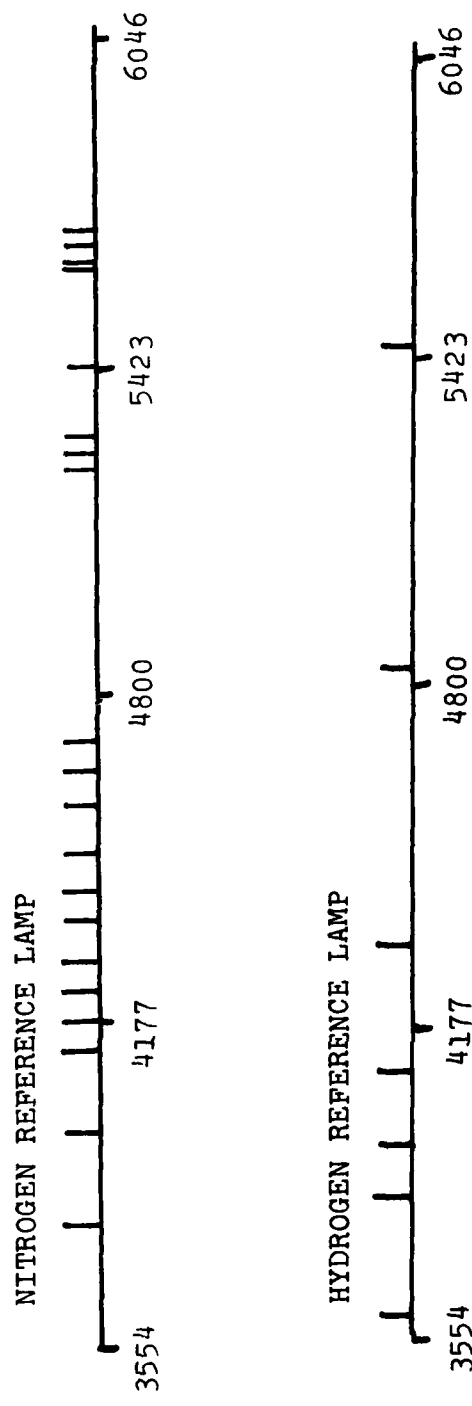
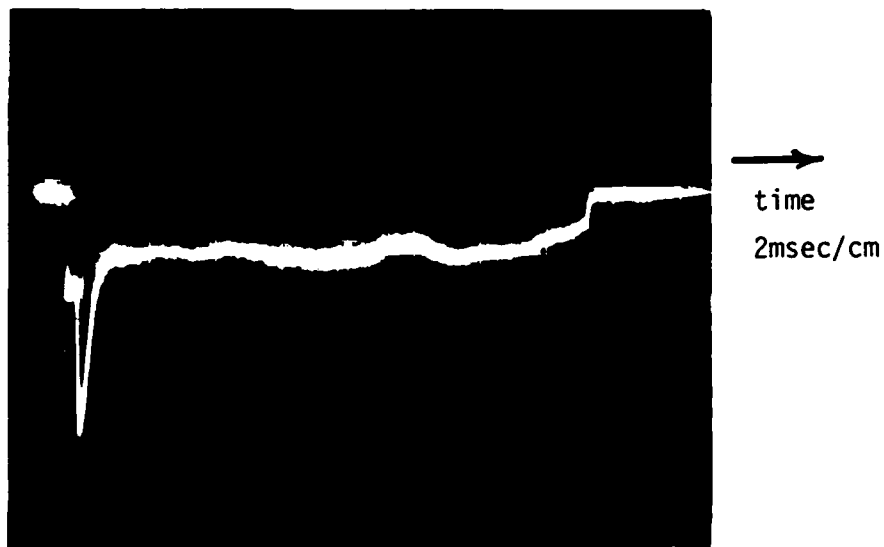


Figure 23. Schematic of Spectral Lines/Bands of Reference Lamps

Intensity
of A10
Band at
4846 Å



Intensity
of
Continuum
at 4500 Å

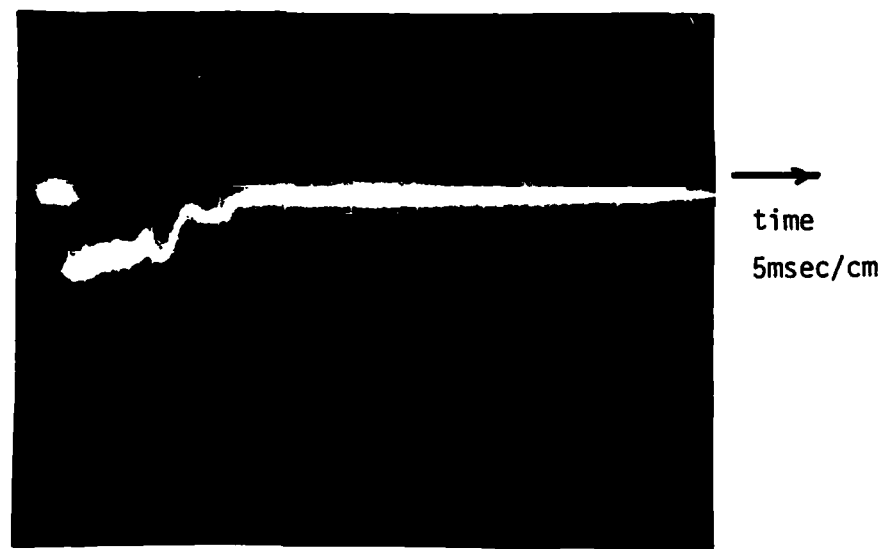
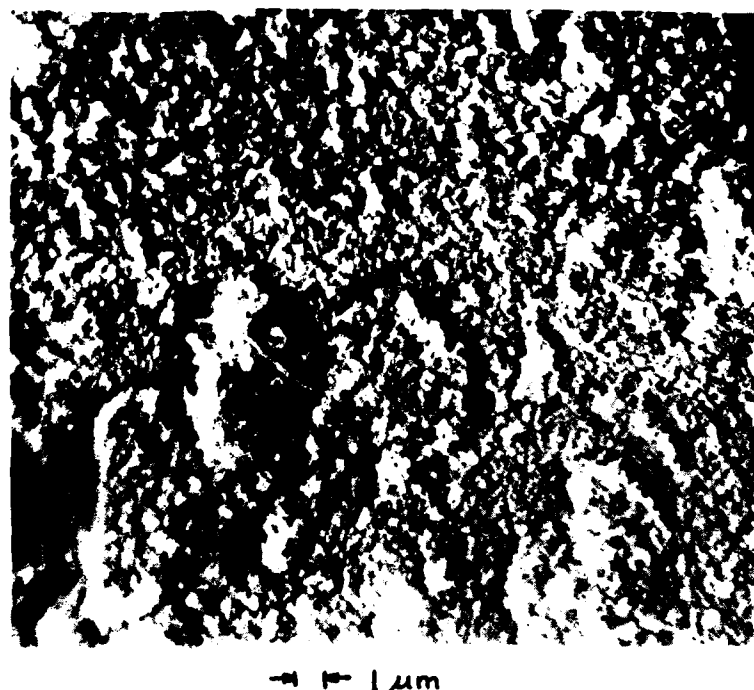


Figure 24. Time History of Emission Spectra



Figure 25. Transmission electron micrograph of Al_2O_3 formed in shank tube.



→ → 1 μ m

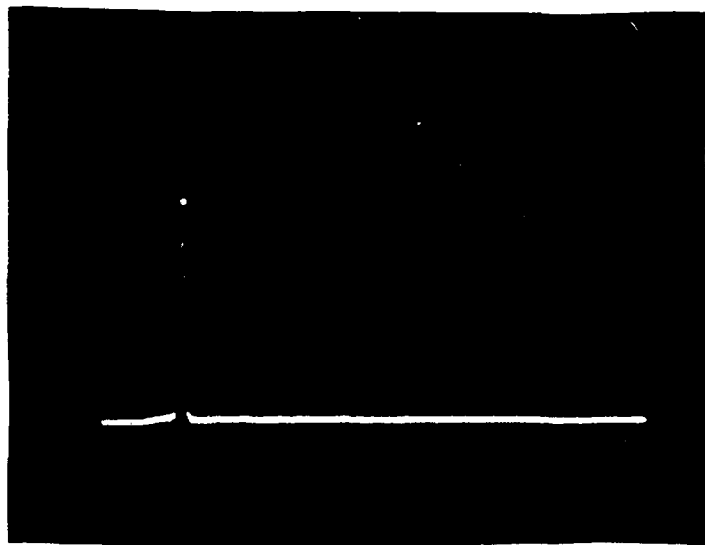


Figure 26. Scanning Electron Micrograph and X-Ray Diffraction Analysis of Solid Products of Combustion

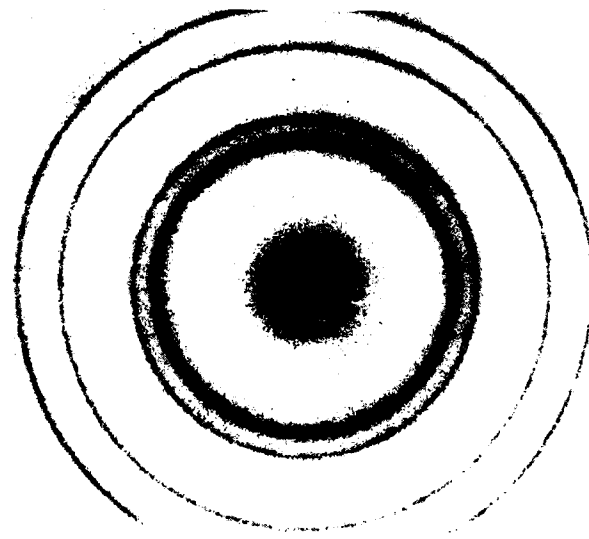
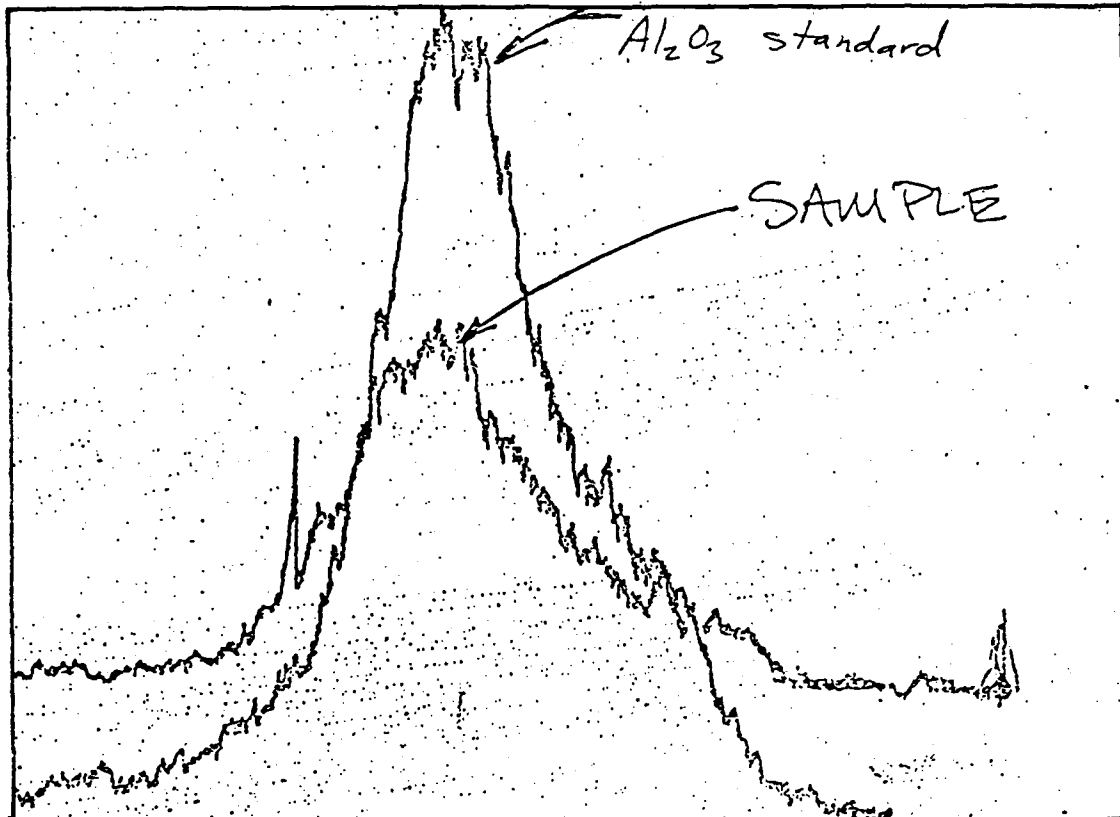
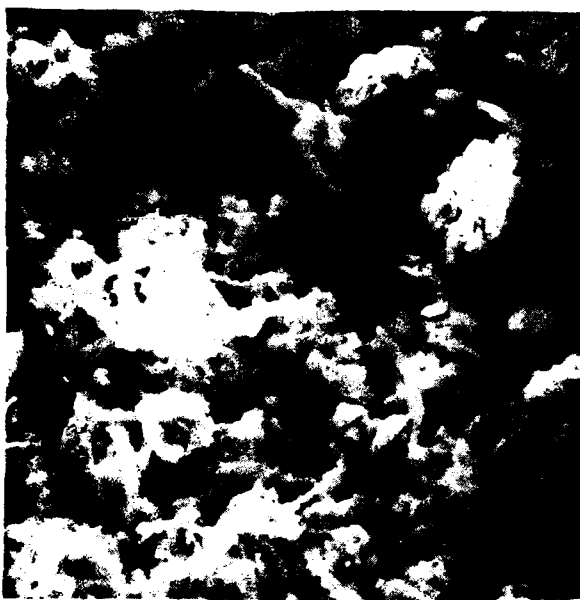


Figure 27. Upper Curve: Analysis of Solid Products of $\text{Al} + \text{N}_2 + \text{H}_2 + \text{O}_2 + \text{Cl}_2$ Reaction Using X-Ray Diffraction, Indicating Presence of Al_2O_3 ; Bottom Photo: Similar Result Using Electron Diffraction.



(a) Electron
Micrograph (600X)

white area = $\text{Al}_2\text{O}_3 + \text{HCl}$

grey area = $\text{Al}_2\text{O}_3 + \text{H}_2\text{O}$



(b) X-Ray Analysis

Aluminum Chlorine Iron Copper
Silicon Chromium / /

Figure 28. Electron Micrograph and X-Ray Diffraction Analysis
of Products of $\text{Al} + \text{N}_2 + \text{H}_2 + \text{Cl}_2 + \text{O}_2$ Reaction



Figure 29. Magnified View (1500X) of Al₂O₃ Particles
in a Region Identified to Also Contain HCl

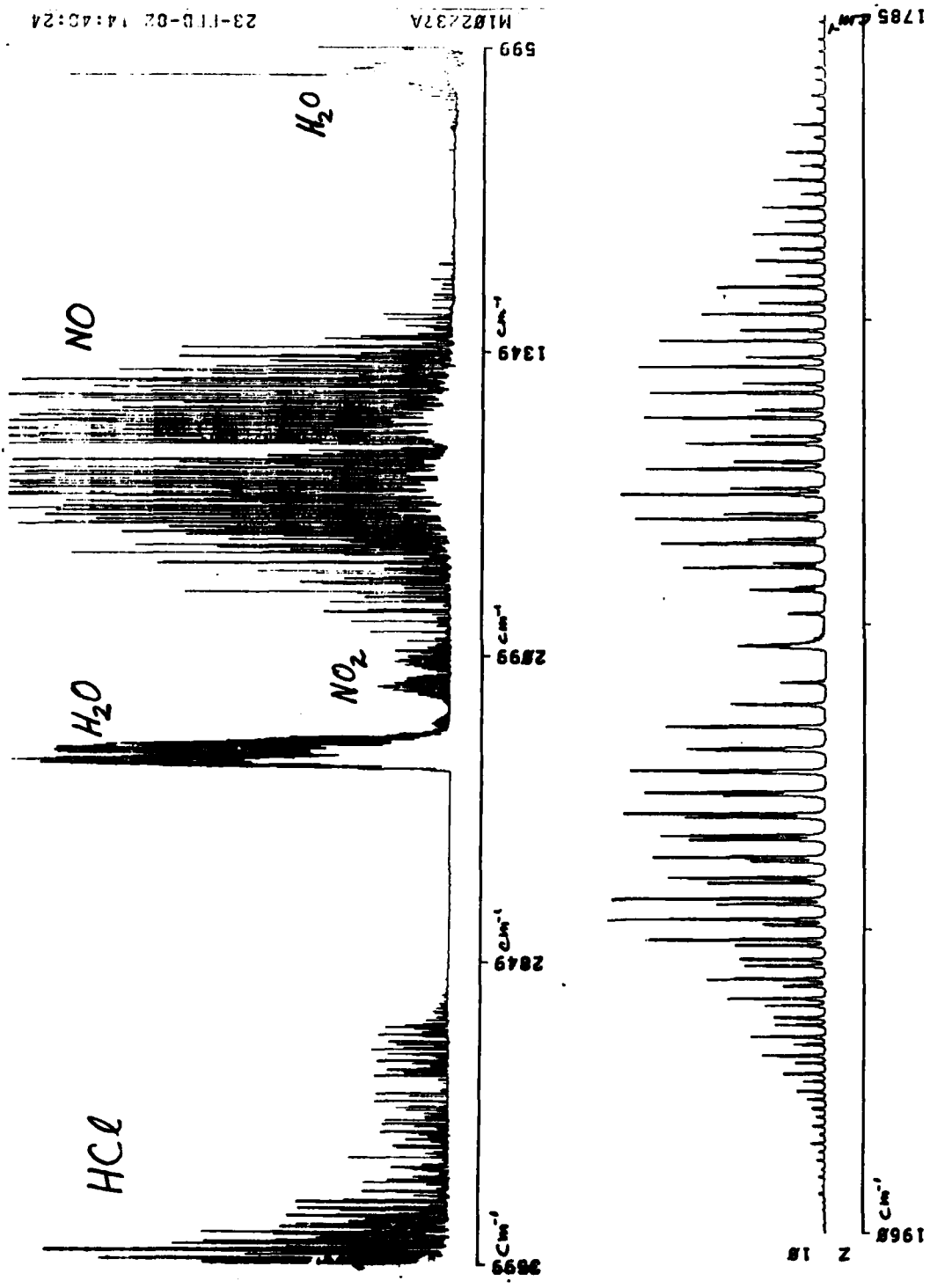


Figure 30. Infrared Spectrometer Analysis of Gaseous Products of Combustion